

Spring 2005

Ambulatory biopotential measurement

Lakshmi Chitra Penugonda
New Jersey Institute of Technology

Follow this and additional works at: <https://digitalcommons.njit.edu/theses>



Part of the [Biomedical Engineering and Bioengineering Commons](#)

Recommended Citation

Penugonda, Lakshmi Chitra, "Ambulatory biopotential measurement" (2005). *Theses*. 482.
<https://digitalcommons.njit.edu/theses/482>

This Thesis is brought to you for free and open access by the Theses and Dissertations at Digital Commons @ NJIT. It has been accepted for inclusion in Theses by an authorized administrator of Digital Commons @ NJIT. For more information, please contact digitalcommons@njit.edu.

Copyright Warning & Restrictions

The copyright law of the United States (Title 17, United States Code) governs the making of photocopies or other reproductions of copyrighted material.

Under certain conditions specified in the law, libraries and archives are authorized to furnish a photocopy or other reproduction. One of these specified conditions is that the photocopy or reproduction is not to be “used for any purpose other than private study, scholarship, or research.” If a user makes a request for, or later uses, a photocopy or reproduction for purposes in excess of “fair use” that user may be liable for copyright infringement,

This institution reserves the right to refuse to accept a copying order if, in its judgment, fulfillment of the order would involve violation of copyright law.

Please Note: The author retains the copyright while the New Jersey Institute of Technology reserves the right to distribute this thesis or dissertation

Printing note: If you do not wish to print this page, then select “Pages from: first page # to: last page #” on the print dialog screen



The Van Houten library has removed some of the personal information and all signatures from the approval page and biographical sketches of theses and dissertations in order to protect the identity of NJIT graduates and faculty.

ABSTRACT

AMBULATORY BIOPOTENTIAL MEASUREMENT

**by
Lakshmi Chitra Penugonda**

Biopotential signals measure the electrical activity of different parts of the body. Conventional bedside monitors only provide information about the body under restricted conditions. Observation and documentation of biopotential signal during daily activities and the relation to patient symptoms may be important factors for clinical decision-making. Ambulatory monitoring helps to monitor the biopotential signal of a patient in the natural environment. The effective ambulatory system can help a physician to diagnose the patient's abnormality.

In this project, a low cost and flexible ambulatory biopotential system, compared to the commercially available systems, was designed and tested. Concurrently a software program was developed for data acquisition and analysis with a Personal Data Assistant (PDA). The data was analyzed in real time using the Lab VIEW PDA. Pilot data was collected using the developed hardware during different normal activities to confirm the accuracy and reliability of the developed hardware and data was collected simultaneously from both a standard ECG machine and the developed system. It was shown that during some activities the system performed as designed, however under extreme conditions where there was more motion artifact, the number of missing R waves increased. The quality of raw ECG from the developed system was as good as the standard ECG during low motion artifact. It has been demonstrated that this newly developed biopotential system is less expensive, flexible, accurate, and more reliable than the commercially available systems and could be used in different clinical and research studies.

AMBULATORY BIOPOTENTIAL MEASUREMENT

by
Lakshmi Chitra Penugonda

**A Thesis
Submitted to the Faculty of
New Jersey Institute of Technology
in Partial Fulfillment of the Requirements for the Degree of
Master of Science in Biomedical Engineering**

Department of Biomedical Engineering

May 2005

Blank Page

APPROVAL PAGE

AMBULATORY BIOPOTENTIAL MEASUREMENT

Lakshmi Chitra Penugonda

Dr. Stanley Reisman, Thesis Advisor Date
Professor of Biomedical Engineering, NJIT

Prof. Michael T. Bergen, Committee Member Date
VA New Jersey Health Care System, East Orange, New Jersey
Adjunct Professor of Biomedical Engineering, NJIT

Dr. Tara Alvarez, Committee Member Date
Assistant Professor of Biomedical Engineering, NJIT

BIOGRAPHICAL SKETCH

Author: Lakshmi Chitra Penugonda

Degree: Master of Science

Date: May 2005

Undergraduate and Graduate Education:

- Master of Science in Biomedical Engineering,
New Jersey Institute of Technology, Newark, NJ, 2005
- Bachelor of Science in Electronics and Instrumentation Engineering,
Sir C R Reddy College Of Engineering, Eluru, AP, India, 2001

Major: Biomedical Engineering

To my beloved husband, father-in-law and family

ACKNOWLEDGMENT

I would like to begin my acknowledgement by thanking Prof. Michael Bergen, who has guided me throughout the project providing valuable and countless resources, insight, and intuition, but also constantly gave me support, encouragement, and reassurance. Without his help, I would not have completed this thesis.

My appreciation to Dr. Stanley Reisman, who has guided me not only in my thesis but also during my graduate studies.

I would like to thank Dr. Tara Alvarez for serving on my thesis committee and giving me valuable suggestions.

Finally, my appreciation to all the members of the Neurobehavioral Research Unit at the Veteran Affairs NJ Health Care System. I would like to thank my husband whose continuous support made even complicated things seem small.

TABLE OF CONTENTS

Chapter	Page
1 INTRODUCTION.....	1
1.1 Objective	1
1.2 Background Information	3
1.2.1 Physiological Measures.....	3
1.2.2 Ambulatory Monitoring.....	14
1.2.3 Introduction to LabVIEW.....	19
2 IMPLEMENTATION.....	21
2.1 General System Overview.....	21
2.2 Hardware Description.....	22
2.2.1 Instrumentation Amplifier.....	22
2.2.2 Sallen-Key Second Order Filter.....	25
2.2.3 DIP Switches.....	29
2.2.4 Inverting Amplifier.....	30
2.2.5 Twin T Notch Filter.....	31
2.2.6 Overall Circuit.....	32
2.3 Software Development and Processing.....	33
2.3.1 Introduction to LabVIEW PDA.....	33
2.3.2 NI DAQcard -6024E (for PCMCIA)	35
2.3.3 iPAQ.....	35

TABLE OF CONTENTS
(Continued)

Chapter	Page
2.3.4 Software Design.....	36
3 SYSTEM VERIFICATION.....	46
3.1 System Testing.....	46
3.1.1 Hardware Testing.....	46
3.1.2 Software Testing.....	48
3.1.3 Pilot Data Collection with the System.....	53
3.2 Data Collection and Processing.....	54
4 RESULTS.....	55
4.1 Heart Rate Analysis for Different Tasks.....	55
4.2 Comparison of Standard and Ambulatory ECG.....	62
4.3 Cost Analysis of the Developed System.....	69
4.4 Memory Capabilities.....	70
5 DISCUSSION	71
6 CONCLUSIONS AND FUTURE DEVELOPMENT.....	73
REFERENCES	75

LIST OF TABLES

Table	Page
2.1 Frequency Settings for Different Biopotential Signals.....	28
3.1 Locations and Amplitudes for ECG Data1	49
3.2 Locations and Amplitudes for ECG Data2.....	50
3.3 Locations and Amplitudes of Large T Wave Data.....	51
3.4 Locations and Amplitudes for Noisy ECG Data.....	52
3.5 Locations and Amplitudes for Noisy ECG Data.....	52
3.6 Activities and Time for Each Activity for Pilot Data Collection.....	54
4.1 Table of Activities	56
4.2 Total and Missing R Waves for all the Subjects	59
4.3 Percentage of Good R Waves.....	60
4.4 Correlation Coefficients for Different Activities.....	62
4.5 Cost Analysis.....	69

LIST OF FIGURES

Figure	Page
1.1 Anatomy of heart.....	3
1.2 Characteristic of electrocardiogram (ECG).....	4
1.3 Calculation of heart rate.....	5
1.4 Anatomy of brain	6
1.5 EEG waves.....	8
1.6 Anatomy of skeletal muscle.....	10
1.7 The parts that can make up a PDA	17
2.1 Block diagram of biopotential system hardware.....	22
2.2 Differential amplifier	23
2.3 Instrumentation amplifier circuit	24
2.4 Gain calculation for instrumentation amplifier.....	25
2.5 Sallen-key low pass filter	25
2.6 Magnitude vs normalized frequency for varying values of Q.....	26
2.7 Sallen-key filter with variable resistors.....	27
2.8 Sallen-Key high pass filter.....	29
2.9 Inverting amplifier circuit.....	30
2.10 Twin T notch filter.....	32
2.11 Hardware design circuit.....	33
2.12 DAQ card.....	35

LIST OF FIGURES
(Continued)

Figure	Page
2.13 iPAQ pocket PC h555.....	36
2.14 Software block diagram.....	36
2.15 Block diagram for data acquisition using LabVIEW PDA.....	38
2.16 Block diagram to create moving window.....	39
2.17 Normal ECG data.....	40
2.18 Second derivative data plot for normal ECG data.....	40
2.19 Noisy ECG data.....	41
2.20 Second derivative plot for noisy ECG data.....	41
2.21 Formula to calculate locations depending on the moving window.....	42
2.22 Block diagram to calculate heart rate.....	43
2.23 Front panel of ECG program.....	44
3.1 High pass filter response for cut-off frequency of 50Hz.....	46
3.2 Frequency response of low pass filter with cut-off frequency 20Hz.....	47
3.3 Frequency response of low pass filter with cut-off frequency 100Hz.....	47
3.4 Frequency response of low pass filter with cut-off frequency 500Hz.....	48
3.5 Frequency response of low pass filter with cut-off frequency 40Hz.....	48
3.6 ECG data1.....	49
3.7 ECG data2.....	50
3.8 ECG with large T wave.....	51
3.9 Noisy ECG data (60Hznoise).....	51

LIST OF FIGURES
(Continued)

Figure	Page
3.10 Noisy ECG data (motion artifact).....	52
4.1 Heart rate plots for different activities for subject1.....	55
4.2 Heart rate plot for different activities.....	57
4.3 Heart rate plots for different activities (continued).....	58
4.4 Plot of percentage of good R waves for different activities.....	61
4.5 Mean and standard error plot for percentage good R waves.....	61
4.6 Correlation coefficients for different activities for four subjects.....	63
4.7 ECG graphs for standard and ambulatory ECG for different activities.....	64
4.8 ECG graphs for standard and ambulatory ECG for different activities (cont.).....	65
4.9 ECG graphs for standard and ambulatory ECG for different activities (cont.).....	66
4.10 ECG graphs for standard and ambulatory ECG for different activities (cont.).....	67
4.11 ECG graphs for standard and ambulatory ECG for different activities (cont.).....	68
4.12 ECG graphs for standard and ambulatory ECG of subject 4 when standing.....	69

CHAPTER 1

INTRODUCTION

1.1 Objective

Observation and documentation of biopotentials during daily activities and the relation to patient symptoms may be important factors for clinical decision-making. Ambulatory monitoring acquires the biopotential signals of patients in the natural environment. Although the laboratory provides control of stimulation and motor activity, it is not typical of a person's ordinary life. The laboratory environment is novel and can induce fear, so any measurements made in it may be poorly generalizable to more natural settings. The laboratory window of observation is limited in time. Infrequent events such as spontaneous panic attacks or cardiac events are easy to miss. Using ambulatory monitoring technology, physiological reactions related to anxiety or other problems can be recorded when and where they happen. Patients with a more situationally-bound type of anxiety would best be assessed by first reviewing the computer diary information and identifying situations that were anxiety provoking, and then by examining the physiological records for these periods. In contrast, patients with more generalized anxiety would best be assessed by looking for a generally elevated activation profile.

The objective of this thesis was to develop a low cost and flexible ambulatory biopotential system compared to the commercially available ambulatory systems in the market, that could collect electrocardiogram (ECG) data, calculate real time heart rate for up to 24 hours and perform data analysis to quantify the quality of raw ECG and heart rate data during different activities, and to design the filters for measuring other

biopotential signals such as the electroencephalogram (EEG), electromyogram (EMG), electrooculogram (EOG), and electrogastrogram (EGG). The acquired ECG data was analyzed in real time and the heart rate as well as raw ECG data was stored on the PDA, which could further be used for clinical research.

A software program was developed using the Laboratory Virtual Instrument Engineering Workbench (LabVIEW) PDA program for data acquisition and analysis [1] of ECG. Reliability and signal quality were considered carefully and verified.

Though the primary goal was to record ECG, the hardware component has the capability of recording many biopotential signals. Adding flexible filter settings, the user can make quick changes to filter and amplifier settings to select between five physiological signals ECG, EEG, EMG, EOG, EGG, which were picked up from the surface of the body and provide signal conditioning to make the signal suitable for recording.

Pilot data was collected and analyzed primarily to test the hardware and software of the biopotential system while performing different activities. Using the developed system, the electrocardiogram was collected and analyzed under different conditions such as when the person was sitting, standing, climbing and descending the stairs, walking on a treadmill at 1mph, 2mph, 3mph, 4mph, 5mph, stretching vertically, stretching horizontally and jumping to confirm the accuracy and reliability of the developed system. The standard ECG and ambulatory ECG were collected simultaneously under different conditions described above except climbing and descending the stairs to quantify the quality of the raw ECG data.

1.2 Background Information

1.2.1 Physiological Measures

1.2.1.1 Heart. The heart is a pump, which circulates blood through the body [2]. It has two pumps. The right side receives oxygen-poor, nutrient-rich blood from the body and sends it to the lungs where its carbon dioxide is exchanged for oxygen. This oxygen-rich blood arrives at the left side of the heart, which provides the force to propel blood throughout the body.

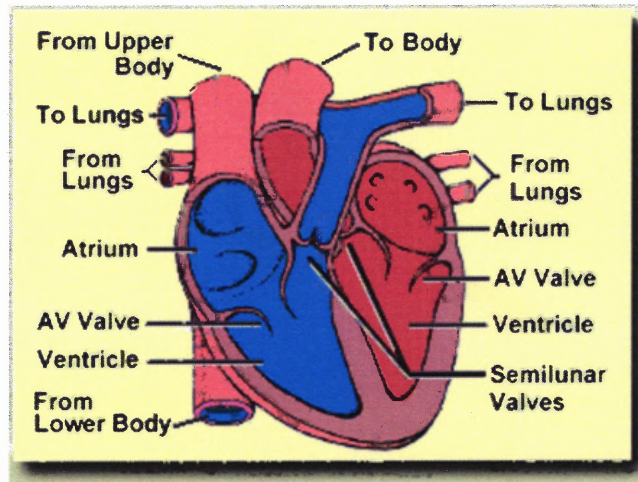


Figure 1.1 Anatomy of heart.

The mammalian heart uses four chambers to circulate blood as shown in Figure 1.1. The left and right halves of the heart each consist of two chambers, an upper atrium which receives the blood from the body or the lungs, and a lower ventricle which forces the blood out of the heart to the lungs or the body. In the normal cardiac cycle, both atria contract simultaneously forcing blood into the two ventricles at the same time. Likewise, both ventricles contract together. In this way, the beating of the heart can be viewed as a two-step process, the upper atria contract followed by the lower ventricles.

1.2.1.2 Electrocardiogram.

An electrocardiogram (ECG) is a graphical representation of the electrical activity of the heart plotted along a time axis [2]. It is the measurement that is recorded at the surface of the skin and is generated by the electrical currents from the cardiac muscle action potentials that causes the contraction of the heart. A typical electrocardiogram as shown in Figure 1.2 consists of regular sequence of waves, the P, QRS, and T waves, each of these waves generated by the specific events in the cardiac cycle. The P wave is generated by the contraction of the atria. The QRS complex is the contraction of the ventricles and the T wave is generated by relaxation of the ventricles. The amplitude of each of these components depends on the orientation of the heart within the individual and the position of the leads (electrodes) used to record the ECG.

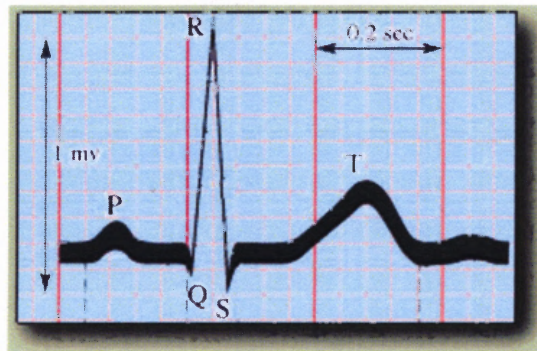


Figure 1.2 Characteristic of electrocardiogram (ECG).

Using a pair of electrodes and a ground electrode, the measurements of the ECG signal are obtained. The differential voltage signal can be measured on the surface of the skin. The locations of the two electrodes differ depending on the desired emphasis on the signal. Because of the size of the QRS complex, if one is only interested in the heart rate, then almost any position of the two electrodes will be sufficient to detect it. Since the

QRS complex is the easiest component of the ECG wave to detect, it is used as the calculation point for the determination of the heart rate.

1.2.1.3 Heart Rate. Heart rate is the number of heartbeats per unit time, usually expressed in beats per minute. The heart rate is based on the number of contractions of the ventricles (the lower chambers of the heart). Because the ECG is plotted along a time axis, the linear distance between neighboring peaks of the simultaneous heartbeats on an ECG corresponds to the time necessary for a single cardiac cycle (heartbeat). The heart rate can be calculated from the time interval between the R peaks of the ECG as mentioned above in Section 1.2.1

$$\text{Heart Rate} = 60 / (\text{R to R interval in seconds}) \quad (1.1)$$

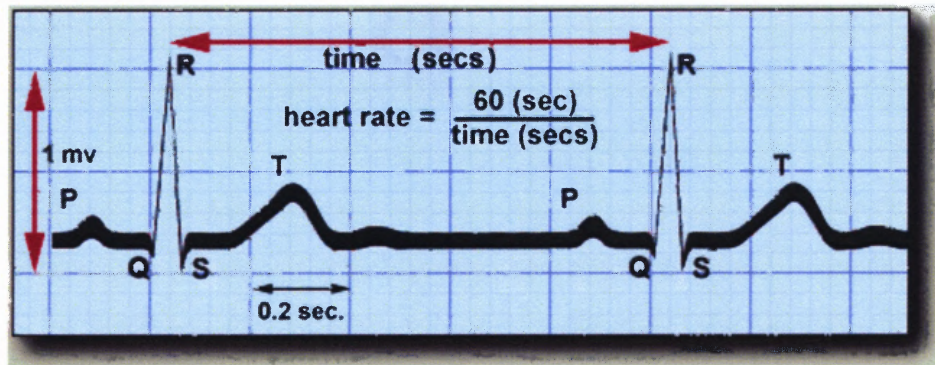


Figure 1.3 Calculation of heart rate.

1.2.1.4 Brain and Electroencephalogram. The human brain is an extremely important organ in the body through which a person is able to respond to various sensory stimuli as well as perform complex activities. Various activities such as cognition, language, sleep, wakefulness, emotions and memory are made possible by the brain. There are many aspects of the human brain that still remain unexplored. The measurement of EEG may provide some information to aid in better understanding of the brain.

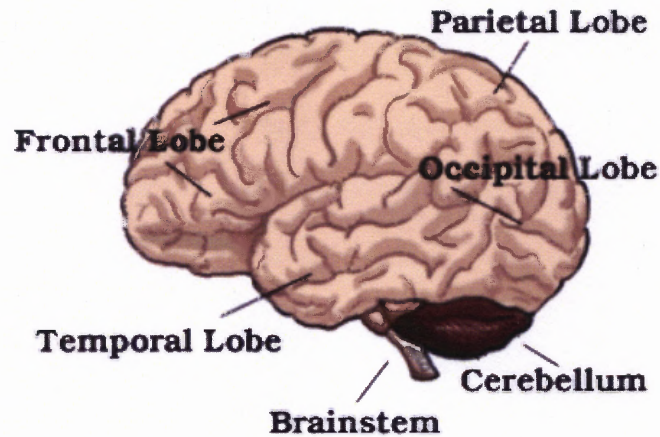


Figure 1.4 Anatomy of brain.

The three main parts of the brain include the brainstem, cerebellum and cerebrum. The brain stem controls vital physiological functions such as breathing, blood pressure and heart rate [3]. The cerebellum receives sensory input from cerebrum and coordinates muscular movement according to motor messages. The cerebrum is an essential part of the brain that controls intelligence, learning, perception, and emotion. The outer layer of the cerebrum in the brain is called cerebral cortex, which contains sensory, motor and association areas. Association areas are located in front of the frontal lobe and in parts of the occipital and temporal node [3]. There are two main types of cells in the cerebral cortex: pyramidal cells and non-pyramidal cells. Non pyramidal cells do not contribute in the generation of EEG. However, the pyramidal cells play a major role in producing the EEG signal. Pyramidal cells consist of a long apical dendrite, which is attached to the cell body on the outer layer of cortex. Any potential changes within the dendrites create potential fields and generate the current. Since the apical dendrite and cell body are connected, the current also flows in the cell body and the entire cell is activated. The cells and dendrites constantly shift their current dipole, strength and orientation, which produce large electric fields (wave like fluctuations) that can be recorded as EEG [4].

The electroencephalogram enables us to measure the electrical activity of the brain noninvasively. An EEG is a record of fluctuations of electric potentials generated by nerve cells in the cerebral cortex. The inherent properties of the cerebral cortex such as understanding perceptual, motor and linguistic abilities can be monitored with this technique [3]. In addition, it is a major tool for diagnosis of many brain diseases and other diseases that are indirectly affected by the brain.

The intensities of the brain waves on the surface of the brain (recorded relative to an indifferent electrode such as earlobe) may be as large as 10mV, whereas those recorded from the scalp have smaller amplitude of approximately 100 μ V. The frequencies of these brain waves range from 0.5 to 100 Hz, and their character is highly dependent on the degree of activity of the cerebral cortex. For example, the waves change markedly between states of wakefulness and sleep. Much of the time, the brain waves are irregular and no general pattern can be observed. Yet, at other times, distinct patterns do occur. Some of these are characteristic of specific abnormalities of the brain, such as epilepsy. Others occur in normal persons and may be classified as belonging to one of the four wave groups (alpha, beta, delta, and gamma).

Alpha waves are rhythmic waves occurring at a frequency between 8 and 13 Hz. They are found in EEGs of almost all normal persons when they are awake in a quiet, resting state of cerebration. These waves occur most intensely in the occipital region but can also be recorded, at times from the parietal and frontal regions of the scalp. Their voltage is approximately 20-200 μ V. When the subject is asleep, the alpha waves disappear completely. When the awake subject's attention is directed to some specific type of mental activity, the alpha waves are replaced by asynchronous waves of higher

frequency but lower amplitude. Figure 1.5 (b) demonstrates the effect on the alpha waves of simply opening the eyes in bright light and then closing them again.

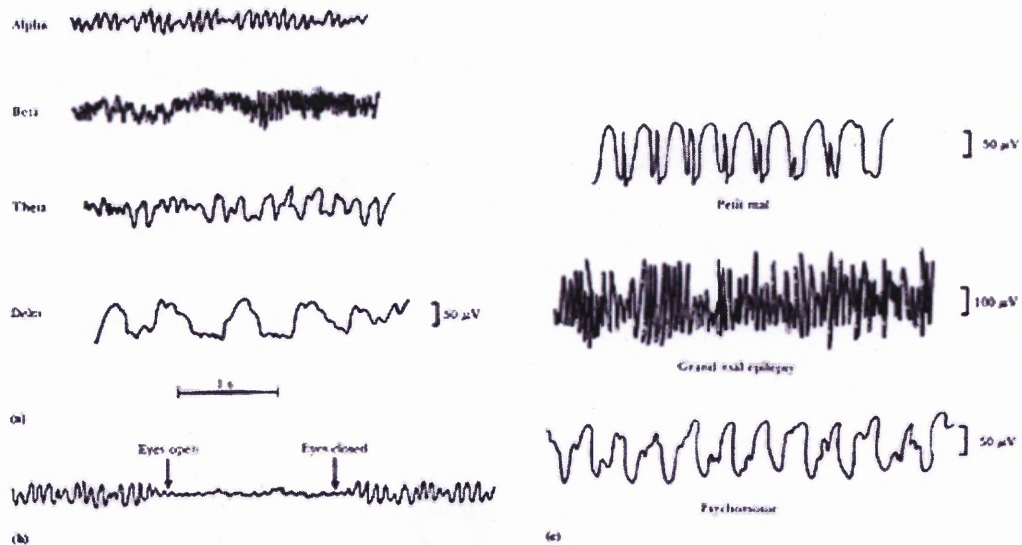


Figure 1.5 (a) Different types of normal EEG waves. (b) Replacement of alpha rhythm by an asynchronous discharge when patient opens eyes (c) Representative abnormal EEG waveforms in different types of epilepsy.

Beta waves normally occur in the frequency range of 14 to 30 Hz, and sometimes- particularly during intense mental activity- as high as 50Hz. These are most frequently recorded from the parietal and frontal regions of the scalp. They can be divided into two major types: beta I and beta II. The beta I waves have a frequency about twice that of an alpha waves. They are affected by mental activity in much the same way as the alpha waves. The beta II waves, on the other hand, appear during intense activation of the central nervous system and during the tension. Thus one type of beta activity is elicited by mental activity, whereas the other inhibited by it.

Theta waves have frequencies between 4 and 7 Hz. These occur mainly in the parietal and temporal regions in children, but they also occur during emotional stress in

some adults, particularly during periods of disappointment and frustration. For example, they can often be brought about in the EEG of a frustrated person by allowing the person to enjoy some pleasant experience and then suddenly removing the element of pleasure. This causes approximately 20s of theta waves.

Delta waves include all waves in the EEG below 3.5 Hz. Sometimes these waves appear only every 2 or 3 sec. They occur in deep sleep, in infancy and in serious organic brain disease. They can also be recorded from the brains of experimental animals that have sub cortical transactions producing a functional separation of the cerebral cortex from the reticular activating system. Delta waves can thus occur solely within the cortex, independent of activities in lower regions of brain.

1.2.1.5 Muscles. Animals use muscles to convert the chemical energy of ATP into mechanical work. Three different kinds of muscles are found in vertebrate animals. Heart muscle, also called cardiac muscle, makes up the wall of the heart [5]. Throughout life, it contracts some 70 times per minute pumping about 5 liters of blood each minute. Smooth muscle is found in the walls of all the hollow organs of the body (except the heart). Its contraction reduces the size of these structures. Thus it regulates the flow of blood in the arteries, moves the breakfast along through your gastrointestinal tract, expels urine from the urinary bladder, sends babies out into the world from the uterus, and regulates the flow of air through the lungs. The contraction of smooth muscle is generally not under voluntary control. Skeletal muscle, as its name implies, is the muscle attached to the skeleton. It is also called striated muscle. The contraction of skeletal muscle is under voluntary control. A single skeletal muscle, such as the triceps muscle, is attached at its origin to a large area of bone; in this case, the humerus At its other end, the insertion, it

tapers into a glistening white tendon, which, in this case, is attached to the ulna, one of the bones of the lower arm.

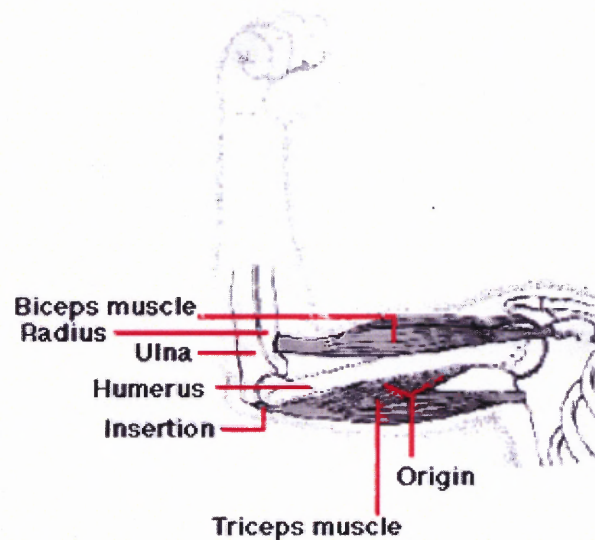


Figure 1.6 Anatomy of skeletal muscle.

As the triceps contract, the insertion is pulled toward the origin and the arm is straightened or extended at the elbow [6]. Thus the triceps is an extensor. Because skeletal muscle exerts force only when it contracts, a second muscle called a flexor is needed to flex or bend the joint. The biceps muscle is the flexor of the lower arm. Together, the biceps and triceps make up an antagonistic pair of muscles. Similar pairs, working antagonistically across other joints, provide for almost all the movement of the skeleton.

Skeletal muscle is made up of thousands of cylindrical muscle fibers often running all the way from origin to insertion. The fibers are bound together by connective tissue through which run blood vessels and nerves. Each muscle fiber contains an array of myofibrils that are stacked lengthwise and run the entire length of the fiber, mitochondria, an extensive endoplasmic reticulum, many nuclei.

1.2.1.6 Electromyogram.

The electromyogram is the recording of the skeletal muscle tension. Skeletal muscle is organized functionally on the basis of the motor unit [4]. The motor unit is the smallest unit that can be activated by a volitional effort, in which case all constituent muscle fibers are activated synchronously. The component fibers of the motor units extend lengthwise in loose bundles along the muscle. In cross section, however the fibers of a given motor unit are interspersed with fibers of other motor units. Thus the component muscle fibers of the single motor unit (SMU) constitute a distributed, unit bioelectric source located in a volume conductor consisting of all other muscle fibers, both active and inactive. The evoked extra cellular field potential from the active fibers of an SMU has a triphasic form of brief duration (3-15ms) and amplitude of 20-2000 μV , depending on the size of motor unit. The frequency of discharge usually varies from 6 to 30 per second.

One of the disadvantages of recording the EMG by using the convenient surface electrodes is that they can be used only with superficial muscles and are sensitive to electrical activity over too wide an area. Various types of monopolar, bipolar and multi polar insertion type electrodes are commonly used in electromyography for recording from deep muscles and from SMUs. These types of electrodes generally record local activity from small regions within the muscle in which they are inserted. Often a simple fine tipped mono polar needle electrode can be used to record SMU field potentials even during powerful voluntary contractions. Bipolar recordings are also employed.

The shape of SMU potentials is considerably modified by disease. In peripheral neuropathies, partial denervation of muscle frequently occurs and is followed by regeneration. Regenerating nerve fibers conduct more slowly than healthy axons. In

addition, in many forms of peripheral neuropathy, the excitability of the neurons is changed and is wide spread slowing nerve conduction. One effect of this is that neural impulses are more difficult to initiate and take longer in transit to the muscle, generally causing scatter or desynchronization in the EMG pattern. Signal processing methods have been employed in EMG analysis, as have automatic techniques for the detection, decomposition, and analysis of EMG signals.

1.2.1.7 Electrooculogram. The electrooculogram (EOG) is a method of recording eye movements and position by measuring the corneal retinal potential of muscles around the eye [4]. Saccadic eye movements are fast eye movements that carry the eyes from one fixation point to another. Smooth pursuit movements are involuntary slow eye movements to follow slowly moving objects. Compensatory movements are smooth involuntary movements to compensate for passive or active movements of the head or the body. Vergence movements are movement of eyes to maintain binocular vision. The EOG signal is one of the easiest to record. The signal is stronger (15 to 200 μ V) with few motion artifacts if the person's head is held still. Eyeblinks can be an artifact but can easily be removed with filters because they are at a different frequency than other biopotential signals. Analysis is also simple. One can measure if eye is moving in correct direction due to a known stimulus.

1.2.1.8 Gastrointestinal System. Digestive systems breakdown and absorb essentially all the digestible food that we put in our mouths [7]. It has been estimated that the human small intestine could absorb as much as 22 pounds of sucrose daily. For the most part, digestion and absorption go to completion, regardless of the needs of the individual. This is not to say that the digestive and absorptive processes do not involve

physiologic regulation. The breakdown and absorption of food proceeds rapidly because a host of regulatory processes tightly regulate the chemical conditions in the gut to optimize conditions for enzymatic and nonenzymatic breakdown of food. An essential aspect of this process is the coordinated movement of food through the digestive system. This involves a variety of negative-feedback regulatory processes. Finally, the absorption of some minerals, vitamins, and water are regulated to a limited extent.

1.2.1.9 Electrogastrogram. An electrogastrogram is similar to an electrocardiogram (ECG) of the heart. It is a recording of the electrical signals that travel through the muscles of the stomach and control the muscles' contraction [8]. It is used when there is a suspicion that the muscles of the stomach or the nerves controlling the muscles are not working normally. Usually this suspicion arises when there is a problem with recurrent nausea and vomiting, signs that the stomach is not emptying food normally. If the electrogastrogram is abnormal, it confirms that the problem probably is with the stomach's muscles or the nerves that control the muscles. The electrogastrogram can be considered an experimental procedure since its exact role in the diagnosis of diseases of the stomach has not been defined yet.

For an electrogastrogram, several electrodes are taped onto the abdomen over the stomach in the same manner as electrodes on the chest for an electrocardiogram. The electrodes sense the electrical signals coming from the stomach's muscles, and the signals are recorded on a computer for analysis. Recordings are made both fasting and after a meal with the patient lying quietly. The study takes two or three hours.

In normal individuals there is a regular electrical rhythm generated by the muscles of the stomach--just as in the heart--and the power (voltage) of the electrical current

increases after the meal. In patients with abnormalities of the muscles or nerves of the stomach, the rhythm often is irregular or there is no post-meal increase in electrical power.

There are no alternatives to the electrogastrogram; however, other studies, like antro-duodenal motility studies or gastric emptying studies may give additional information since abnormal electrical activity of the stomach often results in abnormal muscular activity and reduced emptying of food from the stomach.

1.2.2 Ambulatory Monitoring

Ambulatory monitoring is the measurement of cardiac and physical signals during daily activity. Ambulatory recording of the electrocardiogram (ECG) originated with an American biophysicist, Dr. Norman J. Holter (1914–1983), who developed the recording technology and the ECG monitoring procedure in the 1940s. Dr. Holter's original monitor was a 75-pound backpack containing a reel-to-reel FM tape recorder, analog patient interface electronics and large batteries [9]. The device could record a single ECG lead for several hours and provided the first opportunity for continuous recording and analysis of cardiac electrical activity outside of the health care setting.

Advances in magnetic tape analog signal recording technology led to the development of miniaturized recorders that used standard cassette tapes running at very slow speeds to record up to 24 hours of continuous ECG waveforms from two or three leads. Since technological limitations precluded recording the full 12-lead electrocardiogram, a variant of the standard limb and chest lead placements was developed in an attempt to maximize the efficiency with which cardiac electrical activity

was captured with fewer leads. This led to industry standardization for lead placement for two and three lead analog Holter recorders. The next major advancement in ambulatory ECG recorder technology was the introduction of solid-state recording media to replace the cassette tape mechanisms.

Various media such as Personal Computer Memory Card International Association (PCMCIA) cards, flash memory and EPROM's have been employed to improve the quality and reliability of Holter recorders. This development also facilitated the introduction of extended recording times of up to 48 hours of continuous ECG waveform data. Ambulatory monitoring helps the researcher get a better understanding of the patient symptoms [9]. The recently developed ambulatory systems used a PDA, for which the configuration was modified. The internal battery was removed and an external battery was added which can be used for both the electronics and the PDA. The computer interface was modified to communicate with the electronics and the programs were modified i.e. the PDA can only be used for the purpose of biopotential measurement and is no longer a PDA. There was no memory for the PDA. The external memory was added in order to store the data. With the development of a new era of electronics, the PDA need not be modified in order to build an ambulatory system. It is similar to a small computer that can be programmed as required. The PDA is user friendly with a touch screen, which any person can operate. Ambulatory monitoring can give a large amount of information for patients with medically unexplained symptoms. Development of LabVIEW PDA software made the PDA used for data acquisition applications.

The ambulatory setting has some advantages over the laboratory for assessing the biology of anxiety [10]. Although the laboratory provides control of stimulation and

motor activity, it is not typical of a person's ordinary life. The laboratory environment is novel and can induce fear, so any measurements made in it may be poorly generalizable to more natural settings. The laboratory window of observation is limited in time and infrequent events like spontaneous panic attacks are easy to miss. Using ambulatory monitoring technology, physiological reactions related to anxiety or other problems can be recorded when and where they happen, as well as within the laboratory. Patients with a more situationally-bound type of anxiety would best be assessed by first reviewing the computer diary information and identifying situations that were anxiety provoking, and then by examining the physiological records for these periods. In contrast, patients with more generalized anxiety (for example, post-traumatic stress disorder, and generalized anxiety disorder) would best be assessed by looking for a generally elevated activation profile.

1.2.2.1 Personal Digital Assistant (PDA). The personal digital assistant or PDA is a small hand held computer. The PDA can hold downloaded e-mail, play music and run many applications [11].

In 1996, the original Palm Pilot was introduced, and it was a hit with consumers. It was small and light enough to fit in a shirt pocket, ran for weeks on AAA batteries, was easy to use and could store thousands of contacts, appointments and notes. Today Palm-like devices can be bought from major PC hardware manufacturers (Hewlett-Packard, IBM, Compaq, and Sony). Though originally intended to be simple digital calendars, PDAs have evolved into machines for crunching numbers, playing games or music and downloading information from the Internet. All have one thing in common: They are designed to complement a desktop or laptop computer, not replace one.

PDAs fall into two major categories: hand-held computers and palm-sized computers. The major differences between the two are size, display and mode of data entry. Compared to palm-sized computers, hand-held computers tend to be larger and heavier. They have larger Liquid Crystal Displays (LCD) and use a miniature keyboard, usually in combination with touch-screen technology, for data entry. Palm-sized computers are smaller and lighter. They have smaller LCDs and rely on stylus/touch-screen technology and handwriting recognition programs for data entry.

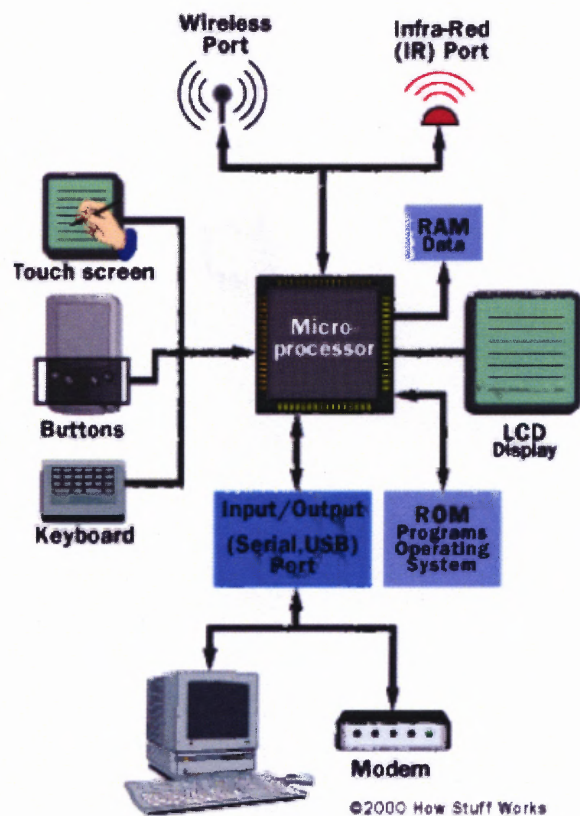


Figure 1.7 The parts that can make up a PDA.

The PDA doesn't have a hard drive. It stores basic programs such as address book, calendar, and memo pad in a read only memory (ROM) chip, which remains intact even when the machine shuts down. The data and any programs added later are stored in the device's RAM. This approach has several advantages over standard PCs. When the PDA

is turned on, all the programs are instantly available. There is no waiting time for applications to load from the hard drive. Any changes made to file are stored automatically. The data is safe even when the device is turned off, since the PDA continues to draw a small amount of power from the batteries.

All PDAs use solid-state memory; some use static RAM and some use flash memory. One megabyte of memory can store up to 4,000 addresses and 100 e-mail messages. However, many application programs take up memory space, so more advanced models usually have more memory (5 to 32 MB). Also, the Pocket PC takes more memory space so PDAs with this operating system usually have 16 or 32 MB. In some PDA models, the amount of memory is upgradeable. The iPAQ hp pocket PC runs on Windows CE 4.2 and has memory capability of 128MB.

1.2.2.2 PCMCIA Card. PCMCIA is a small organization that has developed a standard for small, credit card sized devices called PC cards. Originally these were designed for adding memory to portable computers. The National Instruments DAQCard-6024E brings low-cost high-performance E Series technology to laptop and handheld devices that have a PCMCIA (PC Card) slot [1]. It can sample up to 200 kS/s, 12-bit resolution on 16 single-ended analog inputs. Depending on the hard drive, the NI DAQCard-6024E can stream to disk at rates up to 200 kS/s. It has digital triggering, two 12-bit analog outputs, two 24-bit 20 MHz counter/timers, and eight digital I/O lines. The input range is ± 0.05 to ± 10 V.

1.2.3 Introduction to LabVIEW

Laboratory Virtual Instrument Engineering Workbench (LabVIEW, National Instruments, Austin, TX) is a programming environment in which the user can create programs with graphics. In this regard it differs from traditional text based programming languages like C and Pascal. However, LabVIEW is much more than a language. It is a program development and execution system [1].

LabVIEW executes the program at higher speeds as it is specifically designed to take measurements, analyze data, and present results to the user. Because of LabVIEW's graphical nature, it is inherently a data presentation package. Output appears in many desired forms. Charts, graphs, and user-defined graphics comprise just a fraction of the available output option. The LabVIEW programs are called virtual instruments (VI's) because their appearance and operations imitate actual instruments. Behind the scenes it is analogous to the main programs, functions and subroutines from popular programming languages like C or BASIC.

The VI has two main parts: The front panel is the interactive user interface of the VI, so named because it simulates the front panel of a physical instrument. It can contain knobs, push buttons, graphs and other controls that can be inputted by the user. The Block diagram is the VI's source code constructed in the programming language G. This is the actual executable program. The components are lower level VI's, built in functions, constants and program execution control structures. Front panel objects have corresponding terminals on the block diagram so data can pass from the user to the program and back to the user. In order to use the VI as a subroutine in a block diagram of

another VI, it must have an icon and a connector. A VI used within another VI is called a sub VI and is analogous to a subroutine.

CHAPTER 2

IMPLEMENTATION

2.1 General System Overview

The biopotential signals that could be measured using the developed system were ECG, EEG, EMG, EOG and EGG. ECG and EMG signals were in the order of milli volts. EEG, EGG and EOG signals were in the order of microvolts. These signals were picked up from the surface of the body using biopotential electrodes.

The block diagram of the hardware is shown in Figure 2.1. It consists of an instrumentation amplifier, which was used to amplify the picked up signal. The signal is passed through a high pass filter and then through a low pass filter. A Dual Inline Package (DIP) switch is used in both filters to set the different cut-off frequencies. A notch filter removes the 60Hz noise. An inverting amplifier with different gain settings is further used to amplify the signal. The designed hardware is then interfaced with a PDA using a A/D converter and programmed using the LabVIEW PDA.

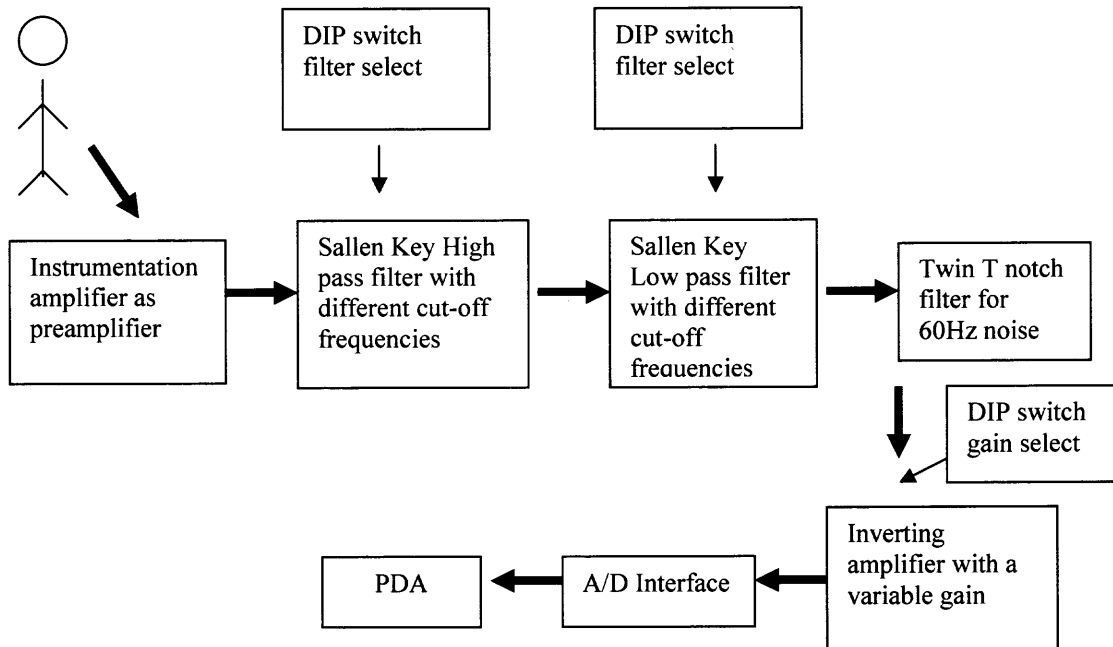


Figure 2.1 Block diagram of biopotential system hardware.

2.2 Hardware Description

2.2.1 Instrumentation Amplifier

An instrumentation amplifier is a differential op-amp circuit providing high input impedance with ease of gain adjustment through the variation of a single resistor [4]. It is beneficial to be able to adjust the gain of the amplifier circuit without having to change more than one resistor value.

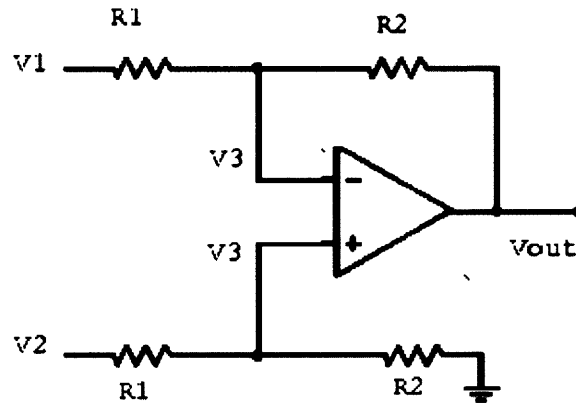


Figure 2.2 Differential amplifier.

The one op-amp differential amplifier is shown in Figure 2.2. If the two inputs are hooked together and driven by a common source, with respect to ground, then the common mode voltage V_c is $V_1 = V_2$. Ideally, the differential amplifier circuit common mode gain G_c is zero. When $V_1 \neq V_2$, the differential voltage ($V_1 - V_2$) produces an amplifier circuit differential gain G_d equal to R_2/R_1 . Common Mode Rejection Ratio (CMRR) is defined as G_d/G_c . This circuit is quite satisfactory for low resistance sources like strain-gage Wheatstone bridges. But the input resistance is too low for high resistance sources. Adding a simple follower to each input provides required buffering. Because this solution uses two additional op amps, gain can be obtained by using a non-inverting amplifier. However, this solution amplifies common mode voltage as well as differential voltage, so there is no increase in CMRR. Hooking up the input resistors of the non-inverting amplifiers and eliminating the connection to ground can increase CMRR. The resulting circuit is shown in Figure 2.3. Assume $V_1 = V_2$, to examine the effects of common mode voltage. V_1 appears at both the negative inputs of the op amps. This places the same voltage at both ends of R_{gain} . The current at resistor R_{gain} is zero. Hence, no current can flow from the op amp inputs. The current through resistors R

between 1 and 3 and 2 and 4 is zero, so V_1 appears at both the op amp outputs and G_c is 1.

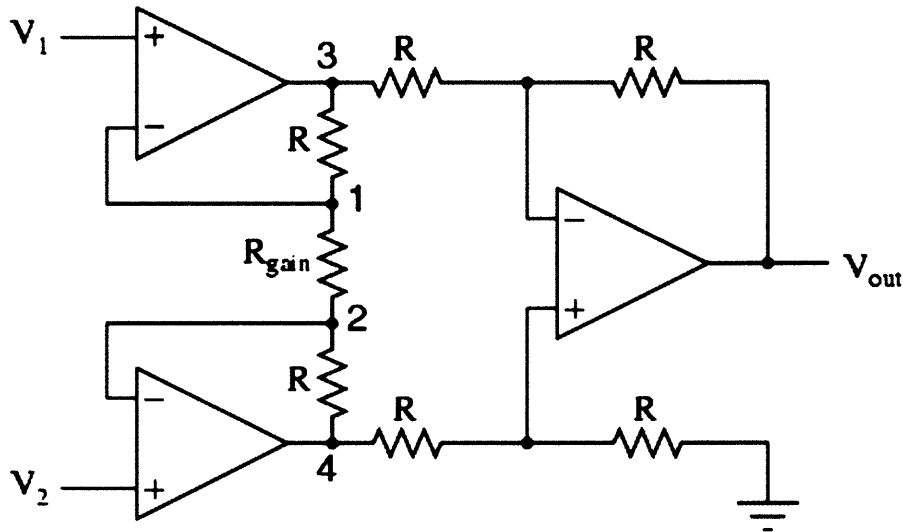


Figure 2.3 Instrumentation amplifier circuit.

When $V_1 \neq V_2$, $V_1 - V_2$ appears across R_{gain} . This causes current to flow through R_{gain} that also flows through the resistors between 3 and 4. Hence the output voltage between 3 and 4 is

$$V = (2R + R_{gain}) * i \quad (2.1)$$

Whereas input voltage between V_1 and V_2 is given by

$$V_1 - V_2 = i * R_{gain} \quad (2.2)$$

The differential gain is then

$$A_v = \left(1 + \frac{2R}{R_{gain}} \right) \quad (2.3)$$

Since the G_c is 1, the CMRR is equal to G_d , which is usually much greater than 1. The circuit has high input impedance, a high CMRR, and a gain that can be changed by adjusting R_{gain} .

An instrumentation amplifier with a gain of 1000 was used as a preamplifier. The ECG signal was on the order of milli volts. The EGG signal was a weak signal on the order of 100 to 800 μ V. EOG was on the order of 15 to 200 μ V, EMG was on the order of 1mV to 50mV and EEG was on the order of 1-10 μ V [12]. A gain of 1000 was used to make the signal suitable for further signal processing. AMP02 (Analog Devices, San Jose, CA) instrumentation amplifier chip was used as a preamplifier. It has a high common mode rejection ratio, high bandwidth and needs a power supply of ± 4.5 V to ± 18 V. The current drawn by the circuit was low, which ensures a long battery life.

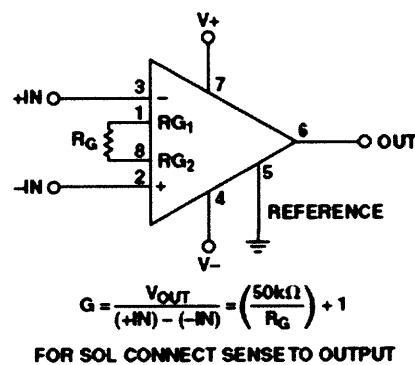


Figure 2.4 Gain calculations for instrumentation amplifier.

To have a gain of 1000, R_g was calculated from Figure 2.4 and chosen as 450 Ω

2.2.2 Sallen-Key Second Order Filter

The Sallen-Key filter is a popular filter due to its versatility and ease of design [13].

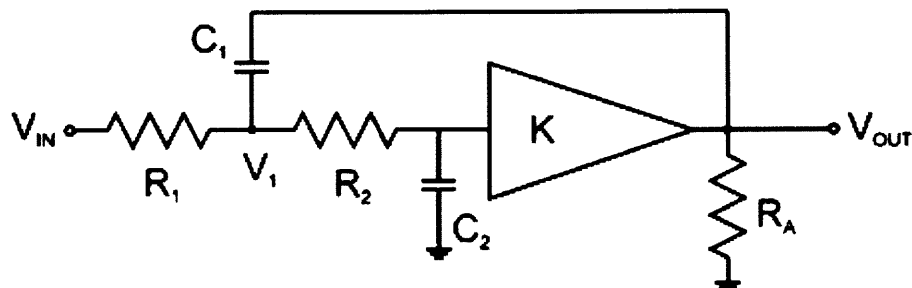


Figure 2.5 Sallen-key low pass filter.

The standard second order filter equation is as follows;

$$\frac{V_{out}}{V_{in}} = K \times \frac{(\omega_o)^2}{s^2 + s\frac{\omega_o}{Q} + (\omega_o)^2} \quad (2.4)$$

Where $\omega_o = 2*\Pi *f_o$ is the cut-off frequency of the filter and Q is the factor that determines the shape of the filter curve.

At low frequencies the result of Equation 2.4 approaches K, since the s terms are small. At high frequencies the result approaches 0, since the s term becomes dominantly large.

Figure 2.6 provides a better understanding of the relationship between Q and ω_o . It shows that the magnitude of the response is equal to Q at ω_o . For a low pass filter the response begins at 1 and then tapers off at higher frequencies. The magnitude of the response at the cut-off frequency is dependent on the Q of the circuit.

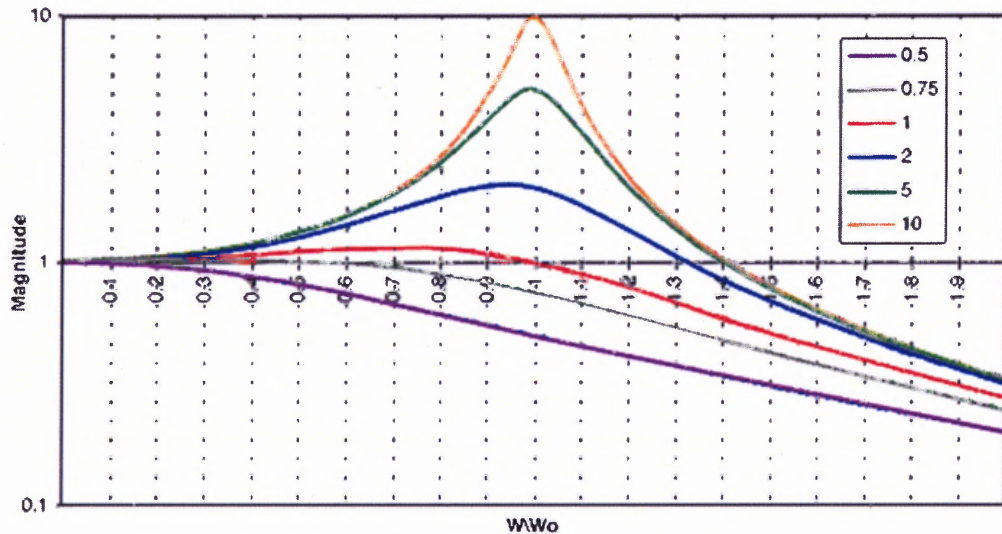


Figure 2.6 Magnitude vs. normalized frequency for varying values of Q.

The equations to solve the filter from Figure 2.5 are;

$$\frac{V_{in} - V_1}{R_1} + \frac{V_{out} - V_1}{\frac{1}{s \times C_1}} + \frac{\frac{V_{out}}{K} - V_1}{R_2} = 0 \quad (2.5)$$

$$\frac{V_1 - \frac{V_{out}}{K}}{R_2} + \frac{0 - \frac{V_{out}}{K}}{\frac{1}{s \times C_2}} = 0 \quad (2.6)$$

Solving Equations 2.5 and 2.6 and eliminating, the equation for the Sallen-Key low pass filter is as follows;

$$\frac{V_{out}}{V_{in}} = K \times \frac{\frac{1}{R_1 \times R_2 \times C_1 \times C_2}}{s^2 + s \left[\frac{1}{R_1 \times C_1} + \frac{1}{R_2 \times C_1} + \frac{1}{R_2 \times C_2} (1-K) \right] + \frac{1}{R_1 \times R_2 \times C_1 \times C_2}} \quad (2.7)$$

Comparing Equation 2.7 with Equation 2.4, the cut-off frequency is given by

$$\omega_0 = \frac{1}{\sqrt{R_1 \times R_2 \times C_1 \times C_2}} \quad (2.8)$$

and Q is given by

$$Q = \frac{1}{\sqrt{\frac{R_2 \times C_2}{R_1 \times C_1} + \frac{R_1 \times C_2}{R_2 \times C_1} + (1-K) \sqrt{\frac{R_1 C_1}{R_2 C_2}}} \quad (2.9)$$

From these equations, there are 5 parameters that can be varied.

To design a low pass filter with a variable crossover frequency and a Q of 0.707 the filter has been refined by adding an op-amp, which is wired for unity gain. It also includes the variable resistors R_2 and R_3 that would be a dual ganged pot so that they remain equal at all times as shown in Figure 2.7.

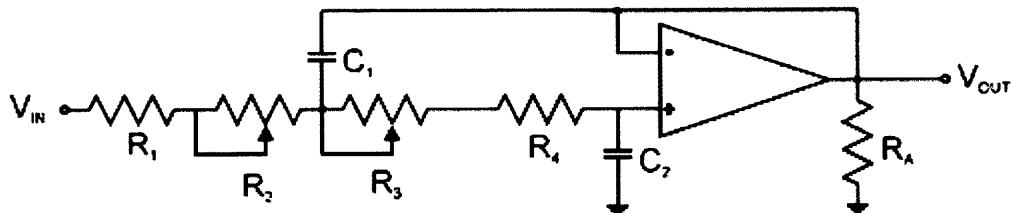


Figure 2.7 Sallen-key filter with variable resistors.

The high pass and low pass filters were designed with different cut-off frequencies for different biopotential signals. The frequency range of ECG was 0.1Hz to 100Hz, for EEG the frequency range was 0.1 to 40 Hz, for EOG the frequency range was 0.1Hz to 20Hz and for EGG the frequency range 0.1Hz to 0.16Hz. EMG1 was the measurement of muscle action near leg or hand muscles which has a frequency range of 0.1Hz to 100Hz. EMG2 was the measurement of muscle action near the heart which has a frequency range of 0.1Hz to 500Hz. EMG3 was the measurement of muscle action for any other muscles which has a frequency range of 50Hz to 500Hz [12]. The frequency ranges of these filters are given in Table 2.1

Table 2.1 Frequency Settings for Different Biopotential Signals

	ECG	EEG	EMG1	EMG2	EMG3	EOG	EGG
High pass cut-off	0.1	0.1	0.1	0.1	50	0.1	0.1
Low pass cut-off	100	40	100	500	500	20	0.16

To design the filter C_1 was set to 0.1 μF . Then C_2 was calculated using

$$C_2 = C_1/4*Q^2 = 0.1\mu\text{F}/4*(\sqrt{2}/2)^2 = 0.05\mu\text{F} \quad (2.10)$$

Now for the frequency of 100Hz for ECG, 40 Hz for EEG, 100Hz for EMG, R was calculated using the following equations

$$R = 1/\omega \cdot \sqrt{C_1 * C_2} = 1/2 * \pi * 100 * \sqrt{0.1\mu\text{F} * 12.5\text{nF}} = 2.2 \text{ K}\Omega \quad (2.11)$$

$$R = 1/\omega \cdot \sqrt{C_1 * C_2} = 1/2 * \pi * 40 * \sqrt{0.1\mu\text{F} * 12.5\text{nF}} = 5.6 \text{ K}\Omega \quad (2.12)$$

$$R = 1/\omega \cdot \sqrt{C_1 * C_2} = 1/2 * \pi * 500 * \sqrt{0.1\mu\text{F} * 12.5\text{nF}} = 450\Omega \quad (2.13)$$

$$R = 1/\omega \cdot \sqrt{C_1 * C_2} = 1/2 * \pi * 20 * \sqrt{0.1\mu\text{F} * 12.5\text{nF}} = 112 \text{ K}\Omega \quad (2.14)$$

This shows that resistors R_1 and R_4 should be around $1.1 \text{ k}\Omega$ for ECG, $2.2 \text{ k}\Omega$ for EEG, 220Ω for EMG and $56 \text{ k}\Omega$ for EOG to set the low frequency limit. The high pass filter was obtained by switching the resistors and capacitors. The circuit is shown in Figure 2.8

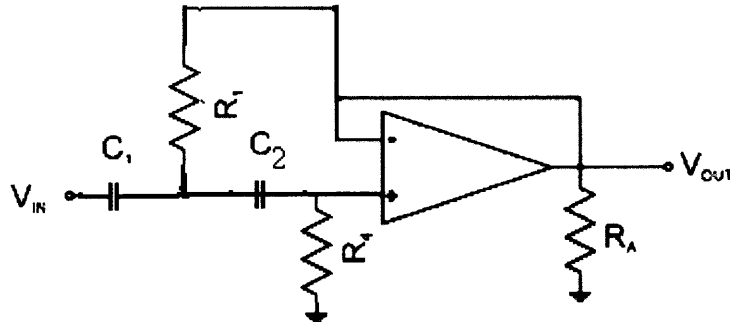


Figure 2.8 Sallen-Key high pass filter.

For the high pass filter the cut-off frequency was chosen as 0.1 and 50. The circuit design has three op amps. To reduce the size of the hardware, a quad op amp, TL074CN (Texas Instruments, Dallas, Texas) was used. It has low input bias and offset currents and has a fast slew rate. The power consumption is minimal and has very low noise. It has high CMRR. The use of quad op amp mainly reduced the power consumption of the circuit.

2.2.3 Dual Inline Package (DIP) Switches

DIP switches are a series of tiny switches built into circuit boards. The housing for the switches, which has the same shape as a chip, is the DIP [14].

DIP switches enable a circuit board to be configured for a particular type of computer or application. DIP switches are always toggle switches and have two possible positions -on or off. These DIP switches are used to switch the filter settings for ECG,

EEG, EMG, EOG and EGG. A series of DIP switches (model EAH 08) was used in the circuit design to set the filter settings and the gain of the amplifier.

2.2.4 Inverting Amplifier

The Figure 2.9 shows an inverting op amp circuit.

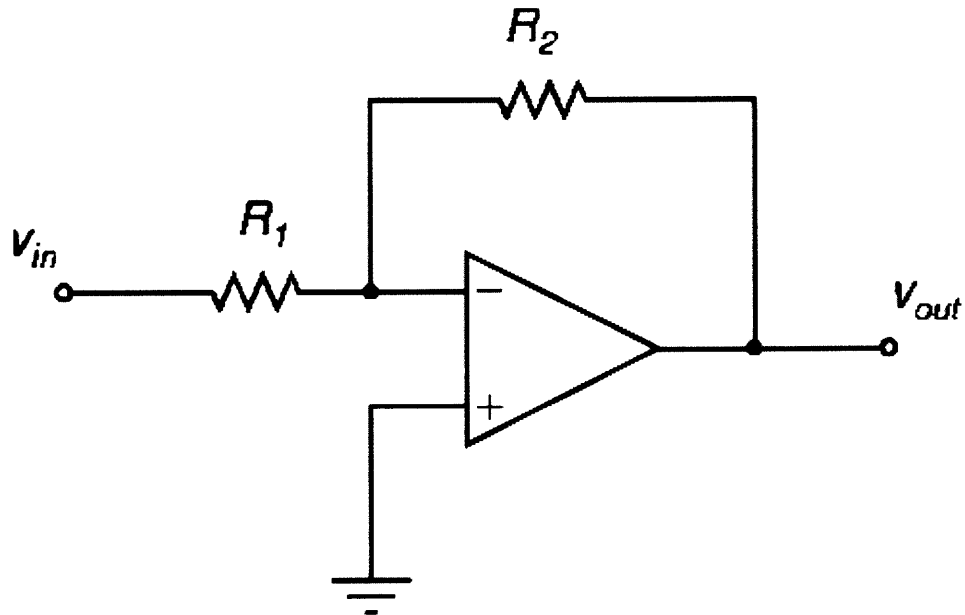


Figure 2.9 Inverting amplifier circuit.

A portion of V_{out} is fed back to the negative input of the op amp. This negative feedback provides the inverting amplifier with many advantages such as increased bandwidth and lower output impedance [4]. The positive input of the op amp is at 0V, so the negative input of the op amp is also at 0V. This condition is called virtual ground. Since R_2 and R_1 form a voltage divider, the feedback voltage will be

$$\text{Feedback voltage} = V_{out} R_2 / (R_1) \quad (2.15)$$

The gain of this circuit, was then calculated as $-(R_2)/R_1$ and was made variable with the help of a DIP switch. The gain could be chosen as 1, 10, 50, and 100 depending on the biopotential signal that was being measured. For ECG the gain of 10 was used

since the signal was in the range of 0.5-4mV. A gain of 50 was used for the EEG signal since it was in the range of 5-300 μ V. Similarly a gain of 100 was used for the EGG signal since it was in the range of 10 to 1000 μ V. For EOG, a gain of 50 was used since the signal was in the range of 50 to 3500 μ V. A gain of 10 was used for EMG since it was in the range of 0.1 to 5mV [12]. These gains were necessary to boost the biopotential signals to the voltage range acceptable for the analog to digital converter NI DAQ 6024E.

2.2.5 Twin T notch Filter

This filter was used to reject or block a frequency or band of frequencies [15]. These filters were often designed into audio and instrumentation systems to eliminate a single frequency, such as 60 Hz. Commercial grade components with 5%-10% tolerance produce a null depth of at least 30 to 40 dB. When the twin-T network is combined with an op amp in a circuit, an active filter can be implemented. The added resistor capacitor network, R2 and C2, work effectively in parallel with the original twin-T network, on the input of the filter. The networks can set the Q of the filter. The op amp is basically connected as a unity gain voltage follower. The Q is found from:

$$Q = R_1/2R_2 = C_1/C_2 \quad (2.16)$$

For a 60 Hz notch filter with a Q of 5, it is usually best to pick the C1 capacitor value and calculate the resistor R1. Let C1= 0.22 μ F. Then R1=12K Ω , R2=120K Ω , C2=0.047 μ F

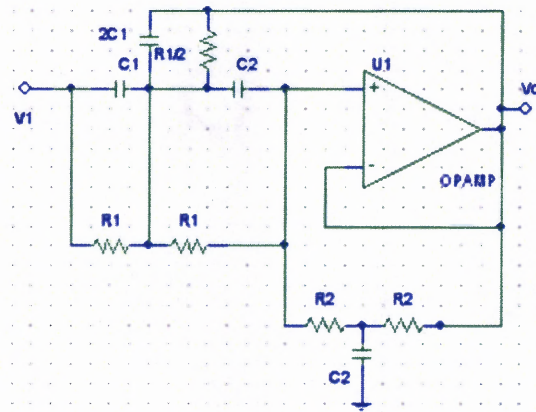


Figure 2.10 Twin T notch filter.

This filter is used to reduce the 60 Hz noise.

2.2.6 Overall Circuit

Figure 2.11 shows the overall circuit. The hardware consists of a preamplifier with a gain of 1000, a high pass filter with adjustable cut-off frequencies of 0.1, 50, low pass filter with cut-off frequencies of 100, 40, 500, 20 and a final amplifier with adjustable gains of 1, 10, 50 and 100. For ECG high pass filter is set to 0.1, low pass filter to cut-off frequency of 100Hz and the final amplifier with a gain of 10. For EEG, the high cut-off is set to 0.1 and low cut-off is set to 40 Hz. For EMG of muscles of hands or legs the high cut-off is set to 0.1 and low cut-off frequency is set to 100 Hz. For muscles near the heart, the high cut-off is set to 50 Hz and low cut-off is set to 500 Hz. For other parts of the body, the high cut-off is set to 0.1 and low cut-off is set to 500 Hz. For EOG the high cut-off is set to 0.1 Hz and low cut-off is set to 500Hz. For EGG, the high cut-off is set to 0.1 Hz and low cut-off is set to 0.16Hz. A notch filter is used to remove the 60Hz noise.

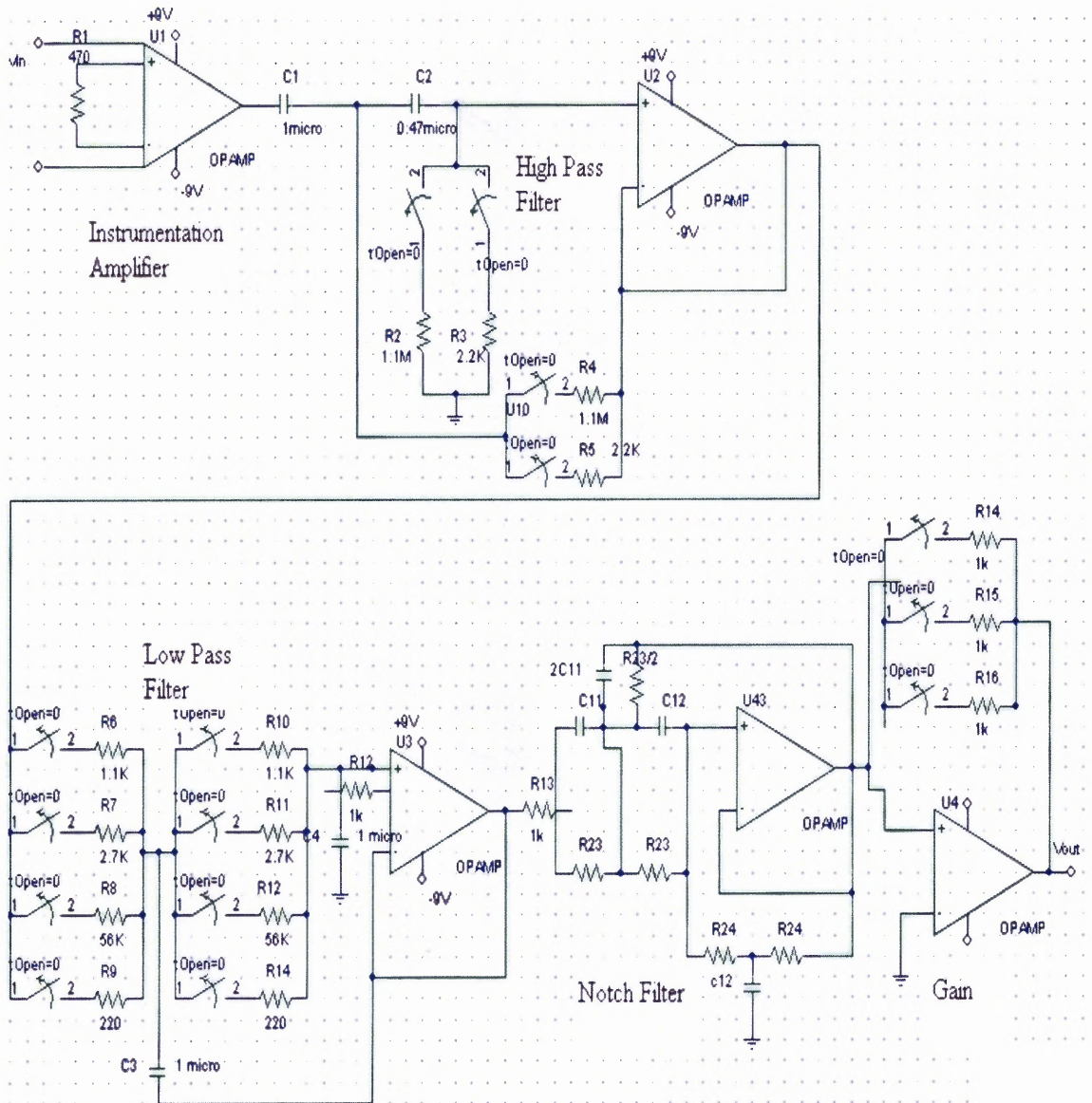


Figure 2.11 Hardware design circuit.

2.3 Software Development and Processing

2.3.1 Introduction to Lab VIEW PDA

Another major part of this project was to write a program using LabVIEW PDA for data acquisition and analysis [1]. The National Instruments LabVIEW PDA Module extends LabVIEW development to applications for PDA handheld devices. The program was

developed in LabVIEW and could easily be downloaded to portable PDA targets. The NI LabVIEW PDA Module automatically compiles VIs to run on selected PDA targets and downloads the completed application to the PDA. The LabVIEW PDA Module modifies the LabVIEW environment to make it easier to build flexible and powerful applications on the PDA, and adds new technology to LabVIEW to optimize applications to run on the smaller memory space and unique processors that are common to PDA's. With LabVIEW PDA technology, NI delivers tools for user-defined, portable solutions for a wide spectrum of applications, such as field test systems, remote control and monitoring systems, and portable data acquisition systems.

The LabVIEW PDA Module also works with the NI DAQCard-6062E, the NI DAQCard-6024E, and the NI DAQCard-6036E. These data acquisition cards use the existing NI hardware to build a new portable data acquisition system. In addition, the LabVIEW PDA module now works with the NI PCMCIA-4050 card to build customized PDA digital multi meter (DMM) devices. The Lab VIEW PDA Module is an add on to Lab VIEW that allows to build applications that run in PDA (Personal Digital Assistant) devices. The PDA module extends the capabilities of Lab VIEW to allow building VIs on the host computer, and then compiling and running the VI on the palm OS or Pocket PC device. Initially the application would be developed using the Lab VIEW on the host computer and then the VI is built for the PDA and the resulting application is downloaded to the PDA device to run the application. PDA VIs were compiled versions of VIs that can be run on a PDA device or emulator. Each PDA VI has a corresponding host VI, which is the VI on the host computer and could be used to build the PDA VI. It

has a front panel, but does not have a block diagram that could be viewed on the PDA device.

2.3.2 NI DAQcard- 6024E (for PCMCIA)

The National Instruments DAQCard-6024E brings low-cost high-performance E Series technology to laptop and handheld devices that have a PCMCIA (PC Card) slot [1]. It can sample up to 200 kS/s, 12-bit resolution on 16 single-ended analog inputs. Depending on the hard drive, the NI DAQCard-6024E can stream to disk at rates up to 200 kS/s. It has digital triggering, two 12-bit analog outputs, two 24-bit 20 MHz counter/timers, and eight digital I/O lines.

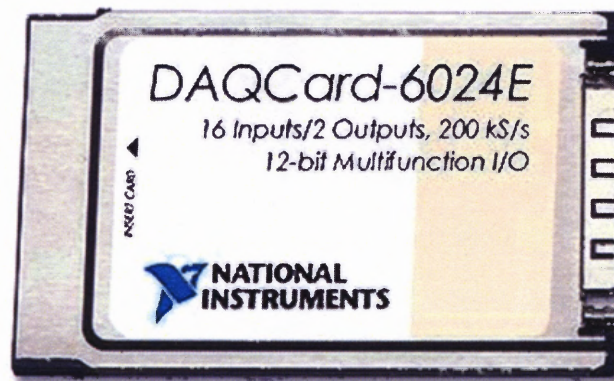


Figure 2.12 DAQ card 6024E.

2.3.3 iPAQ

The iPAQ hp pocket PC is used for analysis and data storage of the ECG data. It has RAM size of 128MB and ROM size of 48MB and provides full PDA functionality with color displays and integrated connectivity options. It supports Bluetooth and runs on Windows CE 4.2 OS. Memory cards up to 512MB could be used for extra storage. The PDA has battery life of 24 hours.

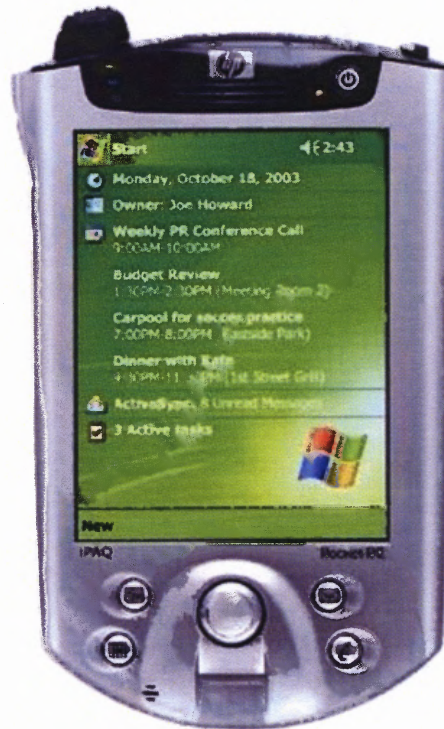


Figure 2.13 iPAQ pocket PC h555.

2.3.4 Software Design

The main software block diagram is shown in Figure 2.14. The raw ECG was collected from the surface of the body using the hardware described in Section 2.2 and the data acquisition was performed using the A/D card. The raw data was then processed to find the locations of the R waves and the R-R interval and the heart rate were calculated. The results were displayed on the front panel and the data was stored in the PDA.

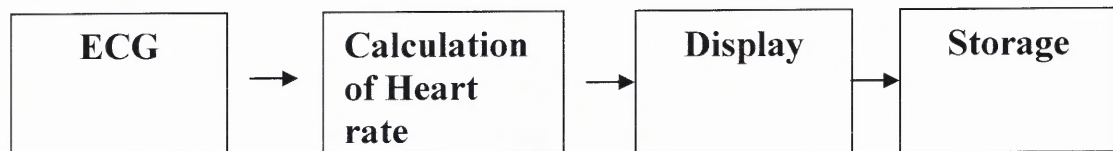


Figure 2.14 Software block diagram.

2.3.4.1 Acquisition of ECG and Signal Processing. The beginning of the program was assembled to set the parameters for the communications between the software and hardware of the system. The ECG data was collected using three electrocardiogram (ECG) electrodes in lead II configuration. The analog output of the designed hardware was fed to the analog to digital converter of the PDA. In the PDA the analog signal was converted to a digital signal at the A/D card or PCMCIA card.

The next VI is DAQmxBase Start Task. It transitions the task to the running state to begin the measurement or generation. This VI is required for all applications in NI-DAQmx Base. It starts the analog input operation and sets up the sampling rate, which is specified by the programmer. Sampling an analog signal involves taking a sample of the signal at discrete times. The rate at which the signal is sampled is known as the sampling frequency. It is typically expressed in samples per second or Hertz. The sampling rate must satisfy the sampling theorem, which states that the sampling rate should be at least twice the highest frequency of the analog signal. In this program, the highest frequency for ECG was 100Hz. Hence the sampling rate was taken as 200 samples/second in order to satisfy the Nyquist criterion. Sampling frequency of more than 200samples/second could be considered but it would require more storage capacity and more processing time.

The DAQmxBaseread.VI was then executed. It reads one or more floating-point samples from a task that contains one or more analog input channels. The block diagram of the data acquisition is shown in Figure 2.15

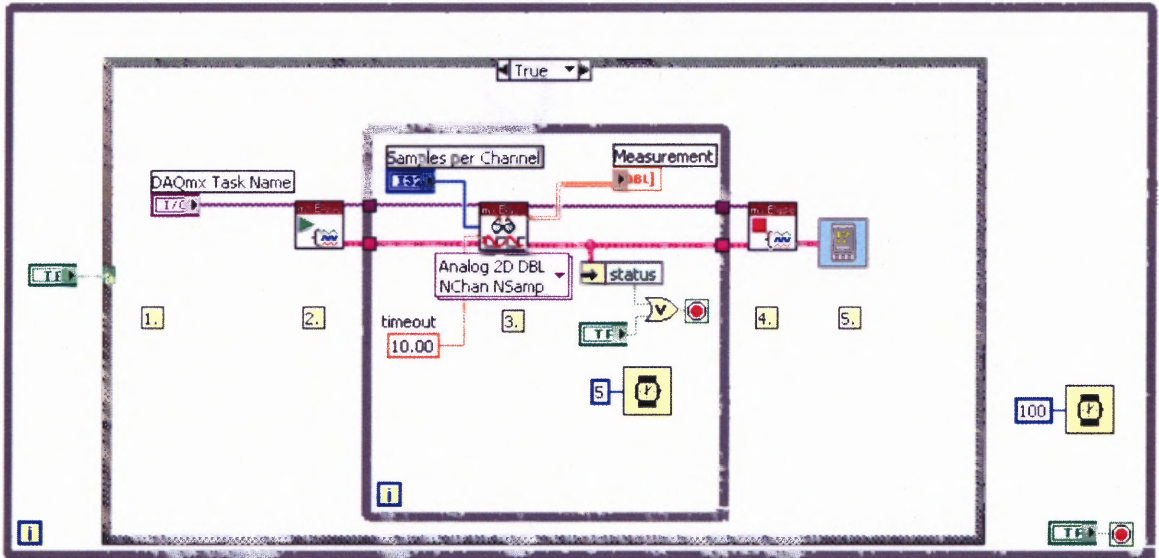


Figure 2.15 Block diagram for data acquisition using LabVIEW PDA.

The raw ECG was used to calculate heart rate. It was first processed to detect the locations and the amplitude of R waves. This process involves taking 200 samples for each channel. 50 samples were taken at a time by applying a moving window through 0 to 50, 25 to 75, and 50 to 100 and so on. The block diagram of the program for applying a moving window is shown in the Figure 2.16.

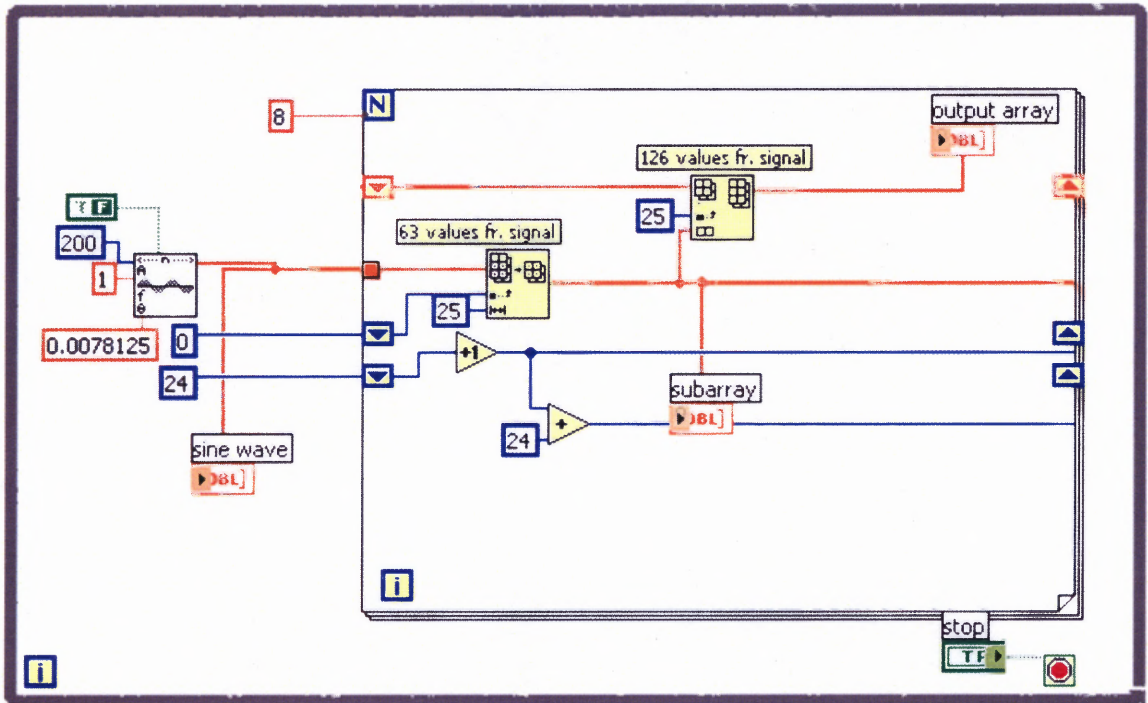


Figure 2.16 Block diagram to create moving window through 0 to 50, 25 to 75, and 50 to 100 and so on upto 150 to 200 samples.

The second derivative was calculated for each set of 50 samples. A change in sign of derivative indicates that there was a peak. The threshold level for the R wave was initially taken as the maximum value of the ECG signal within the first set of 50 samples. The threshold for the next set of 50 samples was then fed back as 0.75 times the previous threshold. The peak was tested to verify if it exceeds the threshold level. Taking 250 samples of ECG data and plotting the raw data and second derivatives verified the conditions to be satisfied for detecting the R waves. The raw data and second derivative plots are shown in Figure 2.17, 2.18.

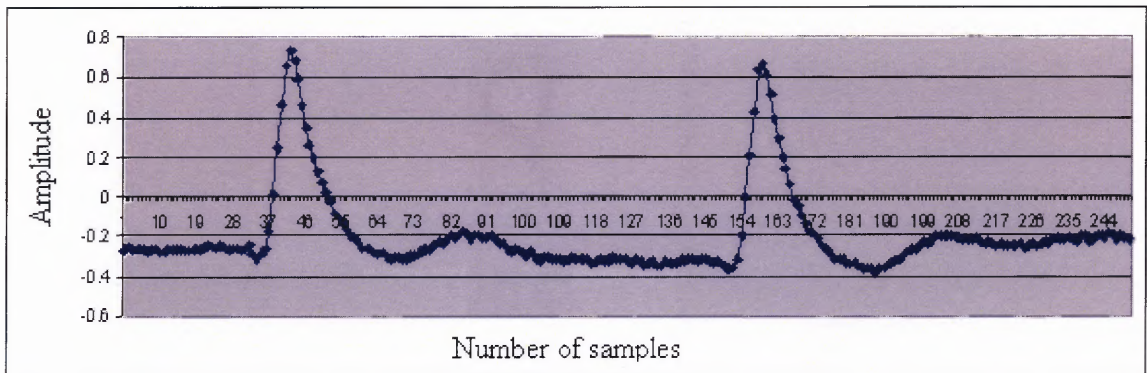


Figure 2.17 Normal ECG data.

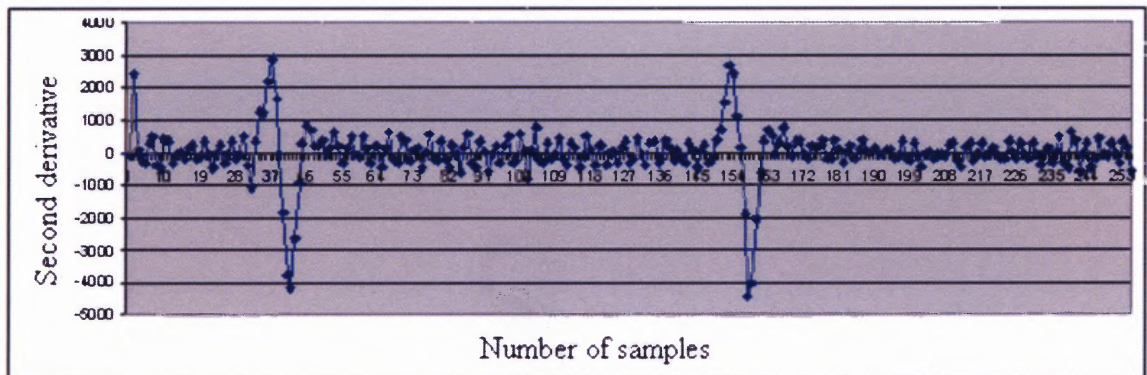


Figure 2.18 Second derivative data plot for normal ECG data.

From these graphs it is confirmed that the R waves were located when the data passes a certain threshold and the second derivative was maximum negative. Another 200 samples of noisy ECG data were taken and the second derivative was plotted to verify the conditions for detection of peaks. The plots are shown in Figures 2.19, 2.20.

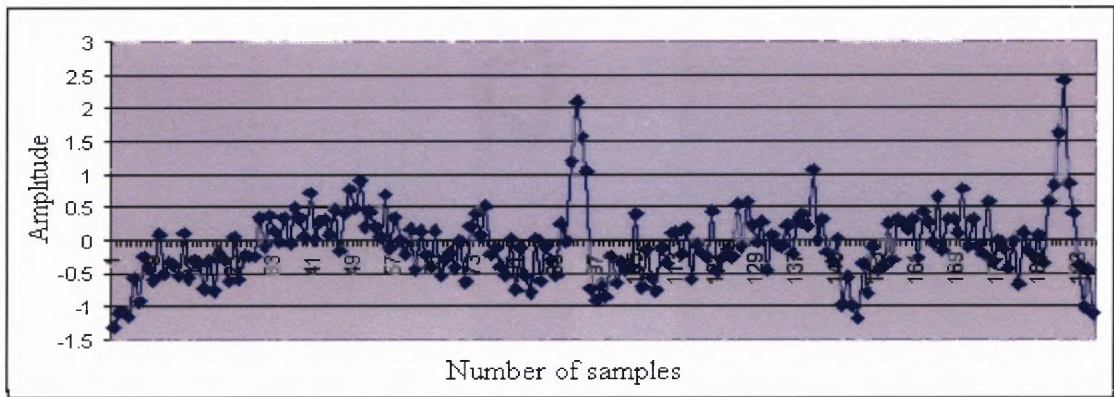


Figure 2.19 Noisy ECG data.

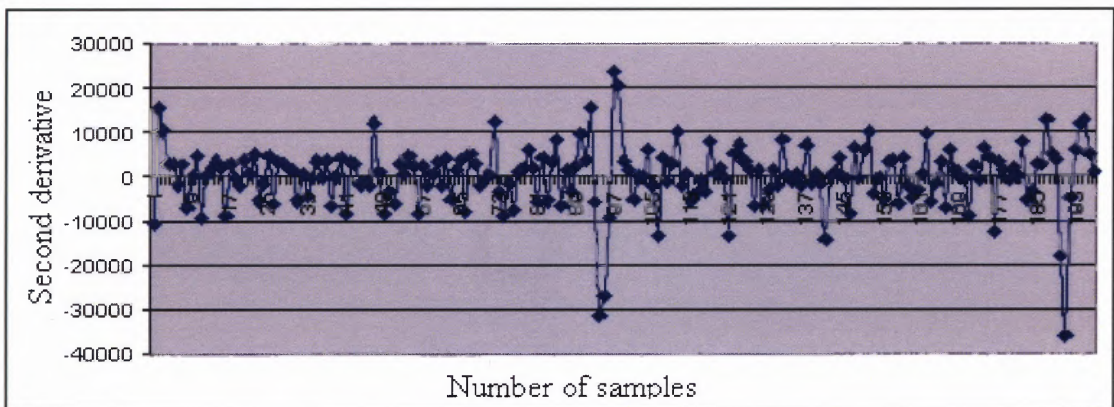


Figure 2.20 Second derivative plot for noisy ECG data.

From these graphs it was confirmed that even in noisy ECG data the R waves were located where the amplitude exceeds a certain threshold and the second derivative was maximum negative.

There were three loops in the program. The outer loop takes 200 samples at a time. These were split into eight sets of 50 moving window samples. These eight sets were 0-50, 25-75, 50-100, 75-125, 100-150, 125-175, 150-200, 175-225 which includes 25 samples from the next set of 200 samples. Therefore, the second loop runs eight times for each set of 200 samples. The third loop was used to traverse through the set of 50

samples. The block diagram to calculate the location of the R wave is shown in Figure 2.21.

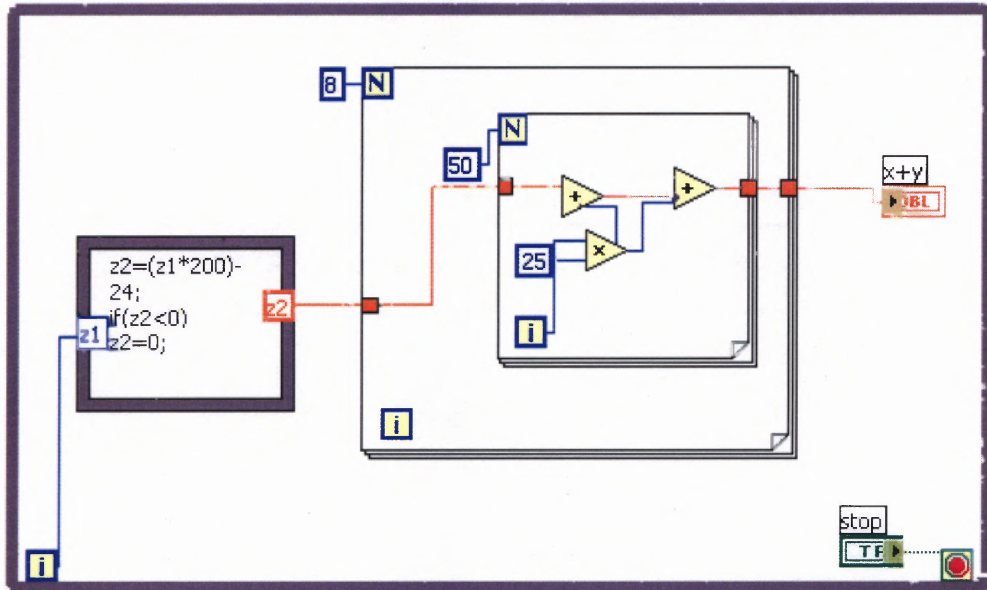


Figure 2.21 Formula to calculate locations depending on the moving window.

$$\text{For } i_1=0, \text{ location of the peak} = i_2*25+i_3 \quad (2.16)$$

$$\text{For } i_1>0, \text{ location} = (i_1*200-24) + i_2*25+i_3 \quad (2.17)$$

where i_1 is the index of the outer loop

i_2 is the index of the second loop

i_3 is the index of the inner loop

The R-R interval is the duration of time between each successive R wave. Using the location of R waves, the R-R interval was calculated in samples between beats.

The block diagram of the program to calculate the heart rate is shown in Figure

2.22

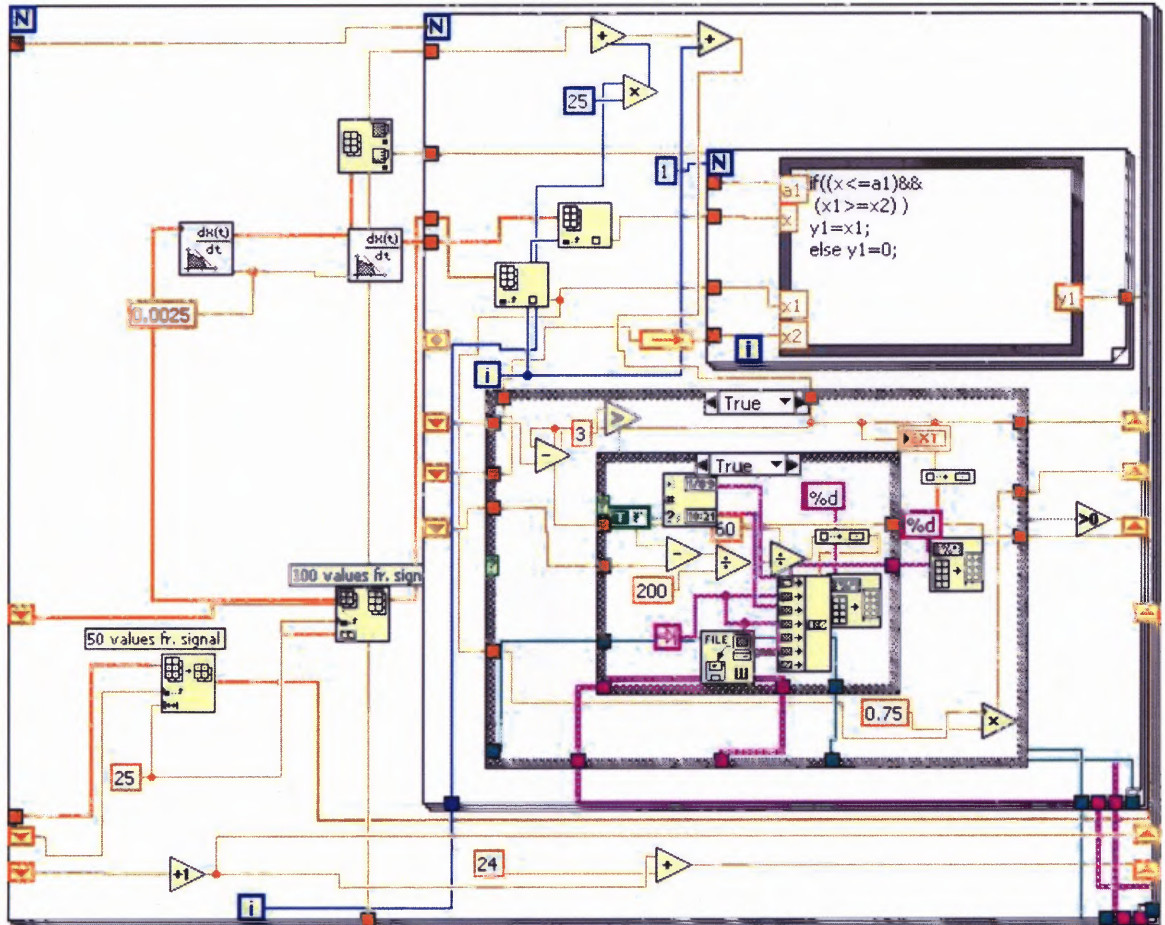


Figure 2.22 Block diagram to calculate heart rate.

The front panel looks like Figure 2.23

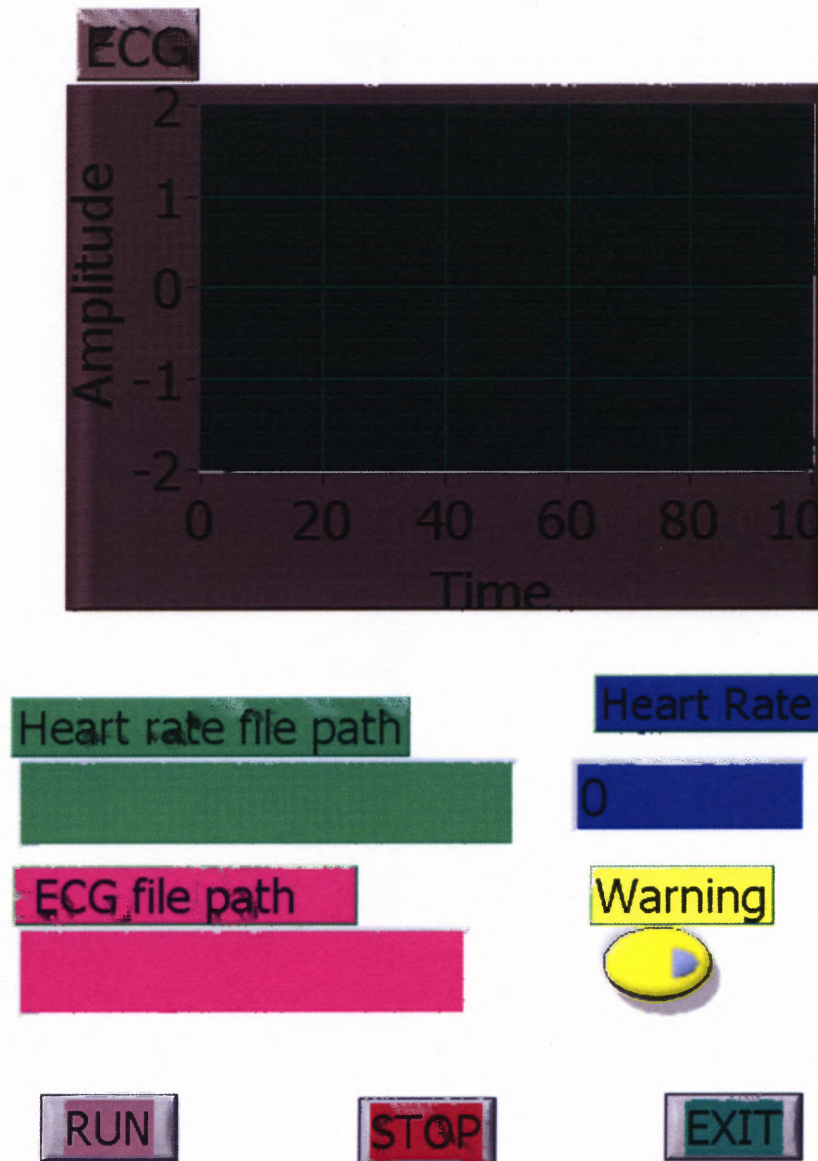


Figure 2.23 Front panel of ECG program.

The Heart rate, in beats per minute was calculated using the following formula:

$$\text{Heart rate} = 60 * (\text{sampling rate} / \text{R-R interval in samples between beats}) \quad (2.18)$$

where the sampling rate was 200 samples/ second as discussed earlier.

2.3.4.2 Acquisition of EEG, EMG, EOG, EGG. The sampling rate for EEG was chosen as 80 samples per second, for EMG, depending on the position of the muscle, the sampling rate is 1000 samples per second near the heart, 200 samples per second for hand or leg muscles, for eye muscles 40 samples per second in order to meet the Nyquist criterion which states that the sampling frequency should be at least two times the highest frequency of the signal.

CHAPTER 3

SYSTEM VERIFICATION

3.1 System Testing

3.1.1 Hardware Testing

The designed hardware was tested using a small sinusoidal input signal of 4mV (up to 2 KHz frequency) to verify the validity of amplification and filter settings. The signal was generated using an attenuator and function generator and the signal was passed through an instrumentation amplifier. The output voltage of the instrumentation amplifier was measured and the gain was calculated and verified to be 1000. The output of the instrumentation amplifier was then connected to a high pass filter. The frequency response of the high pass filter with a cut-off frequency of 50Hz is shown in Figure 3.1

Frequency(Hz)	Gain (dB)
10	-5.57507
20	-3.99145
30	-2.65251
40	-1.49267
50	-0.46962
60	-0.46962
70	0
80	0
90	0
100	0

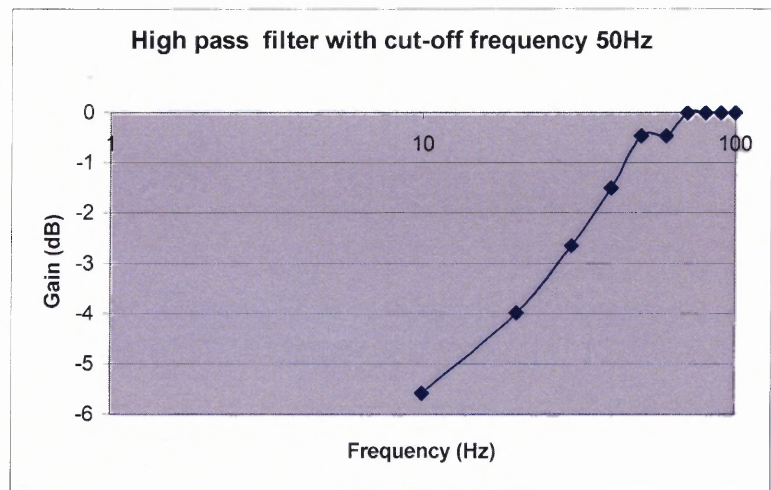


Figure 3.1 High pass filter response for cut-off frequency of 50Hz.

The output of the high pass filter was then passed through the low pass filter. The input signal to the low pass filter was 0.19 V up to 2 KHz frequency. The frequency response for the filter for different cut-off frequencies is shown in Figure 3.2, 3.3, 3.4, 3.5

Frequency (Hz)	Gain (dB)
2	-2.968397
4	-7.513272
6	-11.59567
8	-16.03265
10	-19.55447
12	-22.05325
14	-22.05325
16	-25.57507
18	-23.99145
20	-31.59567
21	-31.59567

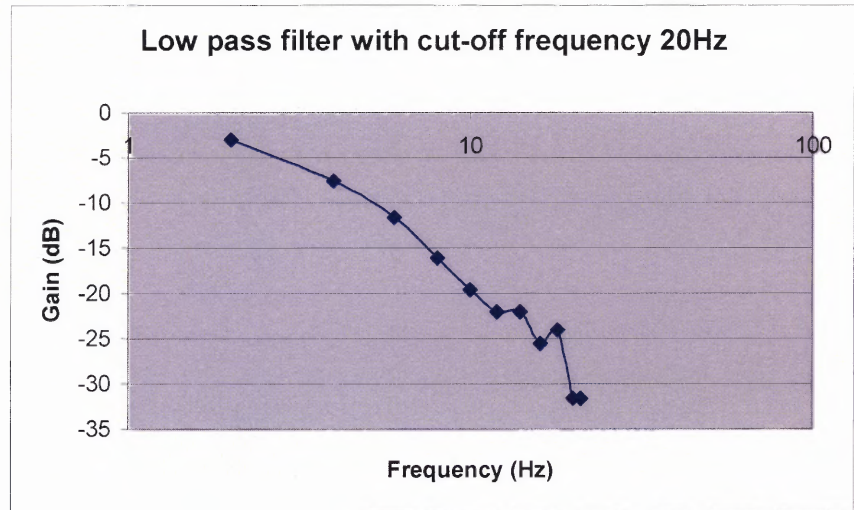


Figure 3.2 Frequency response of low pass filter with cut-off frequency 20Hz.

Frequency (Hz)	Gain (dB)
20	0
40	0
60	-0.714311
80	-1.225393
100	-1.768438
120	-2.347712
140	-2.968397
160	-3.296205
180	-3.991447
200	-4.747218
220	-5.575072
240	-5.575072

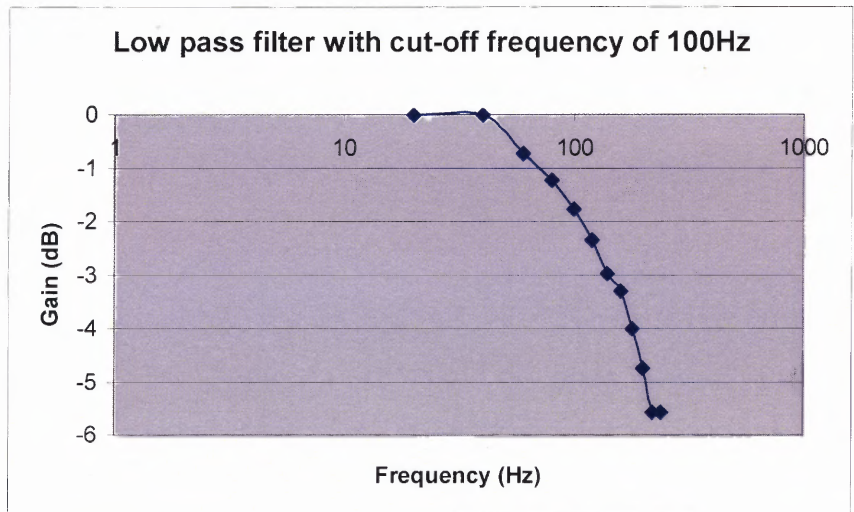


Figure 3.3 Frequency response of low pass filter with cut-off frequency 100Hz.

Frequency (Hz)	Gain (dB)
100	-0.231637
200	-0.714311
300	-1.492672
400	-2.347712
500	-3.296205
600	-4.361115
700	-5.575072
800	-6.986694
900	-8.073847
1000	-9.316805

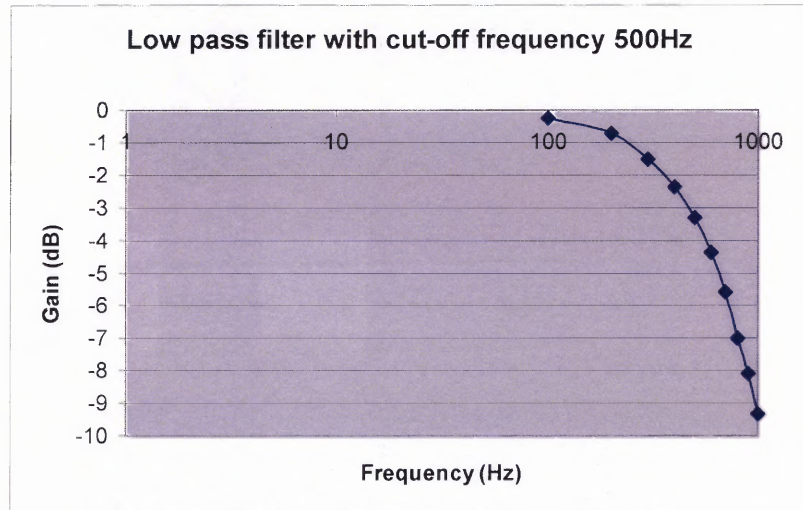


Figure 3.4 Frequency response of low pass filter with cut-off frequency 500Hz.

Frequency (Hz)	Gain (dB)
10	-0.469622
20	-0.714311
30	-1.225393
40	-1.768438
50	-2.347712
60	-3.991447
70	-5.575072
80	-6.490222
90	-8.073847
100	-10.01205

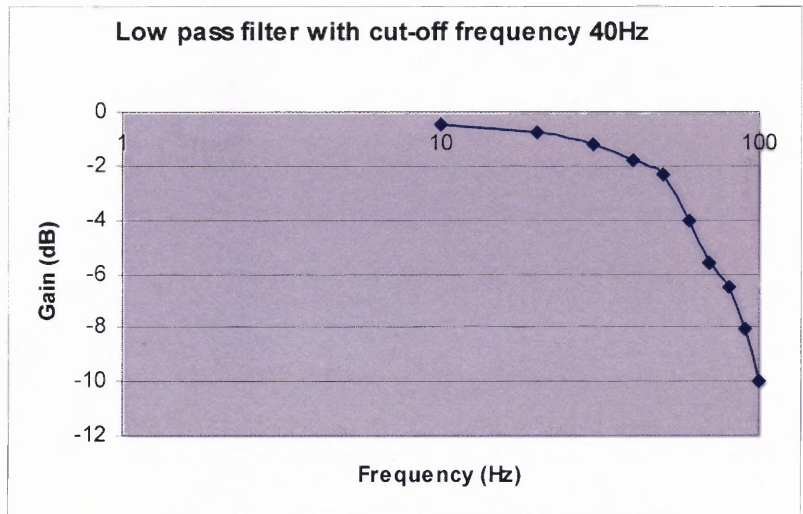


Figure 3.5 Frequency response of low pass filter with cut-off frequency 40Hz.

3.1.2 Software Testing

The LabVIEW PDA program was used to measure the ECG signal and calculate the heart rate.

The ECG program was initially tested using preexisting raw ECG data and the RR intervals and heart rate were calculated for four sets of data. The ECG data from previous experiments at the Veteran Affairs Medical Center, East Orange, NJ were used for testing

the developed LabVIEW PDA software. Clean ECG data while resting was initially used and the software was tested using the data to detect the locations of R waves. The locations of the peaks were identified 100 percent accurately. The amplitude of the peaks was also stored to test the threshold feedback. The locations and amplitudes of the peaks of ECG data shown in Figure 3.6 are shown in Table 3.1

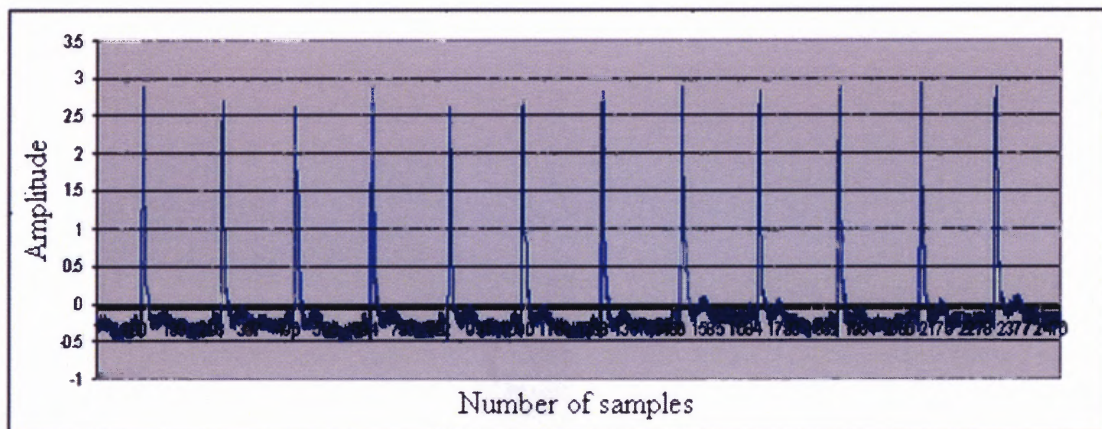


Figure 3.6 ECG data1.

Table 3.1 Locations and Amplitude of ECG Data 1

Loc	120	324	516	713	914	1103	1310	1519	1715	1922
Amp	2.88	2.70	2.60	2.88	2.51	2.54	2.84	2.866	2.836	2.895

A different set of data of a person in the resting state was then taken from the previous experiments at the VA Medical Center and the same procedure was performed. The results are shown in the Table 3.2

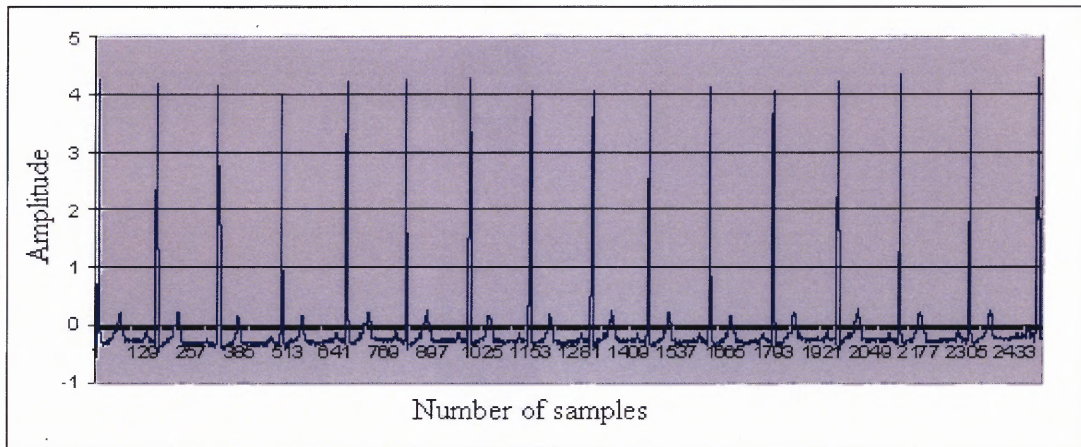


Figure 3.7 ECG data2.

Table 3.2 Locations and Amplitude for ECG Data2

Locations	14	168	327	495	670	827	991	1153	1312	1462
Amplitude	4.27	4.19	4.17	3.920	4.238	4.257	4.316	3.867	4.101	4.091

While analyzing existing ECG data of different subjects in the resting state from the VA Medical Center, ECG data with large T waves was observed. Since the program was working well for normal ECG, it was then tested for this data. The program was 100% accurate in detecting the location of R waves for ECG data with large T waves. The locations and amplitude of peaks of the ECG data shown in Figure 3.8 are shown in Table 3.3

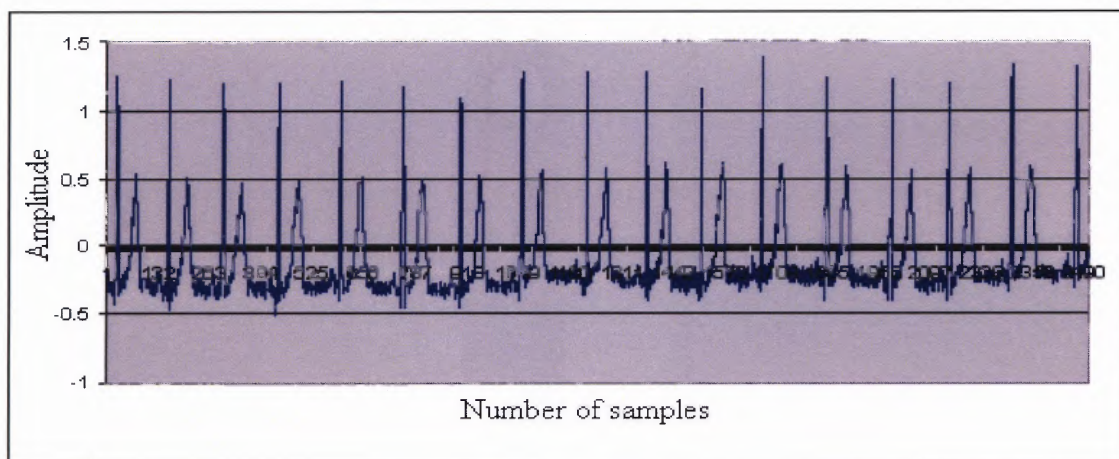


Figure 3.8 ECG with large T wave.

Table 3.3 Locations and Amplitude Of Large T-Waves Data

Locations	26	159	295	440	599	756	905	1060	1220	1373
Amplitude	1.25	1.22	1.19	1.20	1.21	1.15	1.03	1.269	1.279	1.279

Noisy ECG data was next acquired using the developed system and the software was tested. The noisy data was collected with a subject on a treadmill at 3mph. The developed software was able to locate R waves with 100% accuracy. The locations and amplitude of peaks of the ECG data shown in Figure 3.9 are shown in the Table 3.4

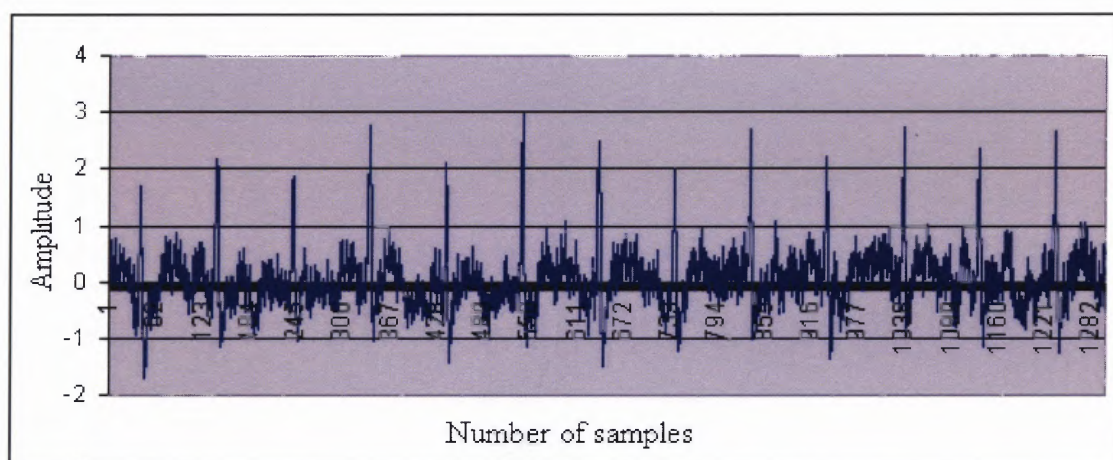
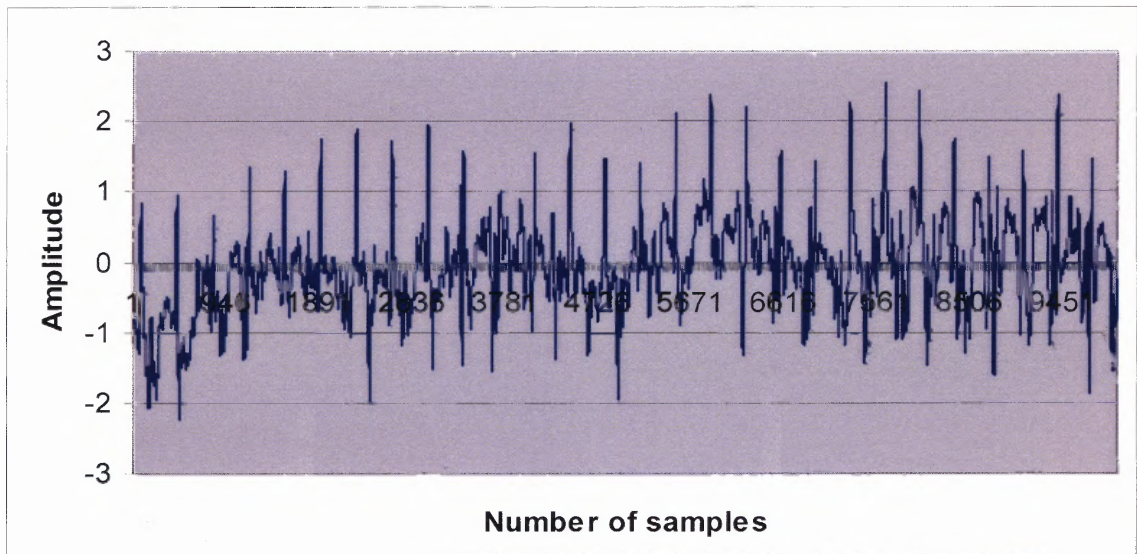


Figure 3.9 Noisy ECG data (60Hz noise).

Table 3.4 Locations and Amplitude of Noisy ECG Data

Locations	43	141	240	340	440	540	640	738	837
Amplitude	1.71	2.182	1.857	2.753	2.104	2.95	2.485	2.0068	2.6831

Noisy data was next collected with a subject on a treadmill at 5mph. The developed software was able to locate R waves with 60% accuracy. Only 17 peaks were detected out of 28 peaks in the data set taken. The locations and amplitude of peaks of the noisy ECG data shown in Figure 3.10 are shown in Table 3.4

**Figure 3.10** Noisy ECG data (motion artifact).**Table 3.5** Locations and Amplitude of Noisy ECG Data

Locations	77	442	1176	1535	1901	2267	2626	3357	4434
Amplitude	0.845	0.962	1.357	1.255	1.724	1.812	1.729	1.577	1.968

These data verify that the software program could locate the peaks 100% accurately for clean data, data with large T wave and noisy data with 60Hz noise and some motion artifact and 60% accurate for noisy data with more motion artifact. The

ECG data, locations of R waves and heart rate were then simultaneously stored in different files to verify the data accuracy.

3.1.3 Pilot Data Collection with the System

Once the hardware and software were working correctly, data were collected from human subjects. Four human subjects, with no history of any disorder were asked to participate in the pilot data collection. Initially the skin was prepared by scratching a part of the stratum corneum using an abrasive pad. The skin was then rubbed with an alcohol swab. The electrode wires were tied together in order to reduce the motion artifact. The ECG electrodes were placed on the body using a lead II configuration and the subject was instructed to sit relaxed, stand, go down stairs, climb stairs, walk on a treadmill at 1mph, 2mph, 3mph, 4mph, 5mph, vertically stretch, horizontally stretch, and jump for 1 minute each. The raw ECG data and the heart rate were stored in the PDA. The heavy activities were performed to test the system with large motion artifact. In order to verify the hardware and the quality of the ECG, raw ECG was collected simultaneously from a standard ECG machine (Model Q4000, Quinton Cardiology Inc, Bothell, WA) and the designed ambulatory biopotential system. This pilot experiment was done on four subjects and the data were analyzed. The list of activities and the time for which each activity was recorded is shown in Table 3.6

Table 3.6 Activities and Time for Each Activity for Pilot Data Collection

Activity	Time in Seconds
Sitting	60
Standing	60
Walking down stairs	60
Climbing stairs	60
Treadmill at 1mph	60
Treadmill at 2 mph	60
Treadmill at 3mph	60
Treadmill at 4 mph	60
Treadmill at 5mph	60
Vertical Stretching	60
Horizontal Stretching	60
Jumping	60

The climbing and descending stairs was not done when testing the hardware simultaneously with a standard ECG. The results will be discussed in Chapter 4.

3.2 Data Collection and Processing

ECG was recorded using the PDA through out the experiment. While acquiring ECG the heart rate was calculated in real time, which was also displayed and recorded. For verifying the hardware, ECG was recorded simultaneously from a standard ECG machine and the designed ambulatory measurement system. After collection of data, the next step was to analyze the data as described in Chapter 4.

CHAPTER 4

RESULTS

4.1 Heart Rate Analysis for Different Tasks

The ECG data were collected from four subjects. Heart rate was calculated in real time. Offline data analysis was performed on a computer using Excel (Microsoft Corporation, Seattle, USA)

The heart rate plot for different activities for subject 1 is shown in Figure 4.1

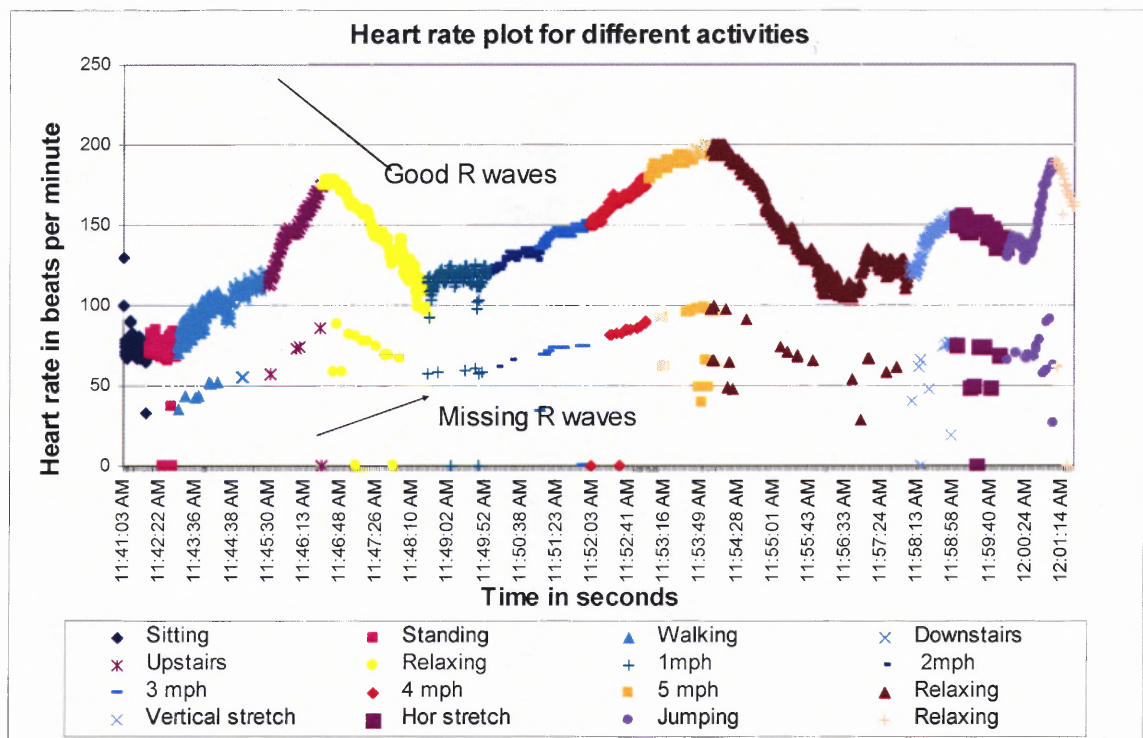


Figure 4.1 Heart rate plots for different activities for subject1.

In Figure 4.1, the representation of good and missing R waves is indicated. The data points that deviated from the graph pattern represent the missing R waves.

The list of activities is shown in the Table 4.1

Table 4.1 Table of Activities

No	Activity	Time in Seconds
1	Sitting	1-60
2	Standing	61-120
3	Walking	121-210
4	Walking down stairs	211-270
5	Climbing stairs	270-330
6	Relaxing	331-450
7	Treadmill at 1mph	451-540
8	Treadmill at 2 mph	541-600
9	Treadmill at 3mph	601-660
10	Treadmill at 4 mph	661-720
11	Treadmill at 5mph	721-780
12	Relaxing	781-1020
13	Vertical Stretching	1021-1080
14	Horizontal Stretching	1080-1140
15	Jumping	1200
16	Relaxing	1200-1260

From Figure 4.1 the heart rate was varying with the intensity of activity. When climbing upstairs and being on a treadmill at 4mph and 5mph the heart rate was high and then the heart rate gradually decreased when relaxing. The heart rate plots for all the stages individually are shown in Figure 4.2, 4.3

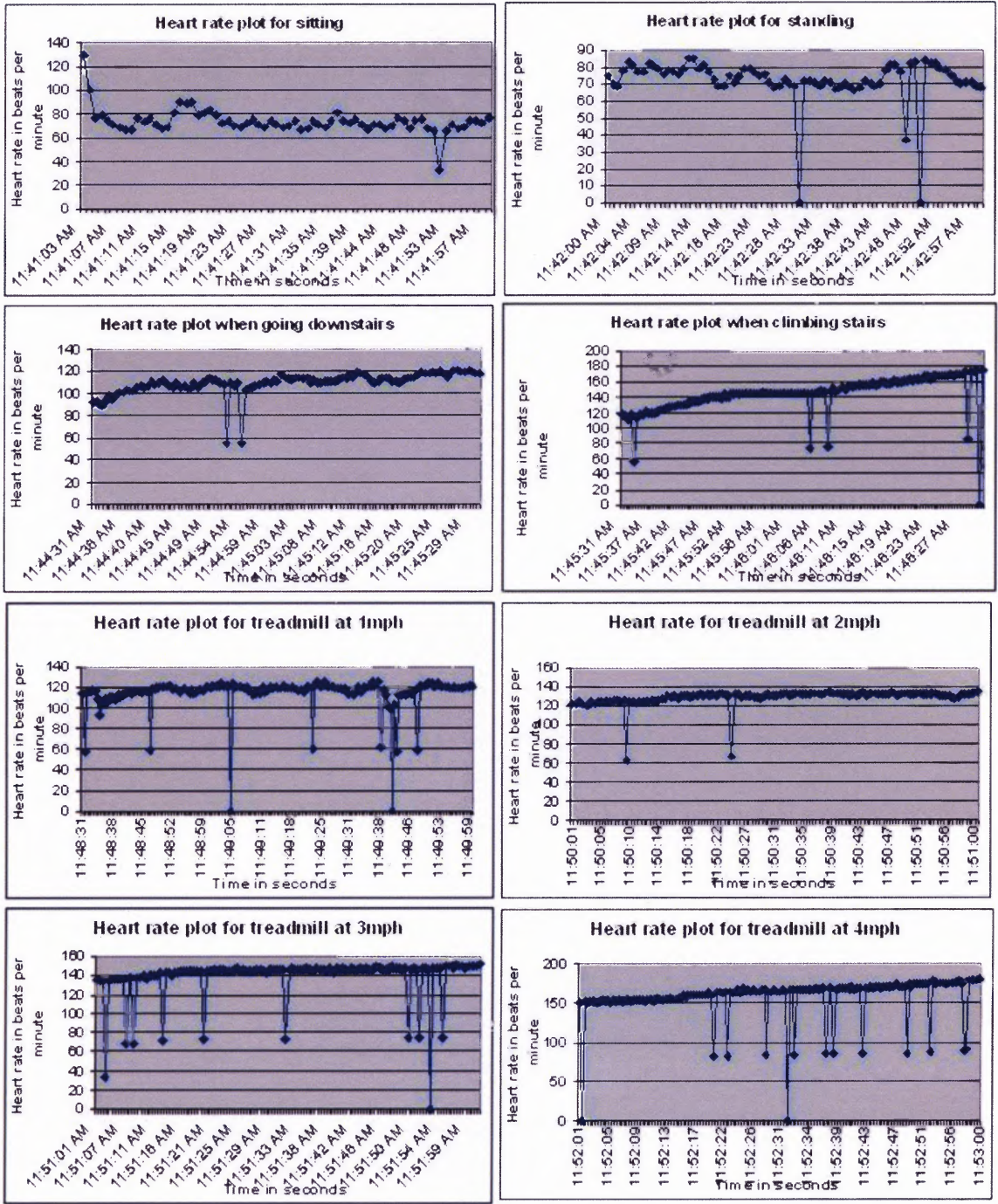


Figure 4.2 Heart rate plot for different activities.

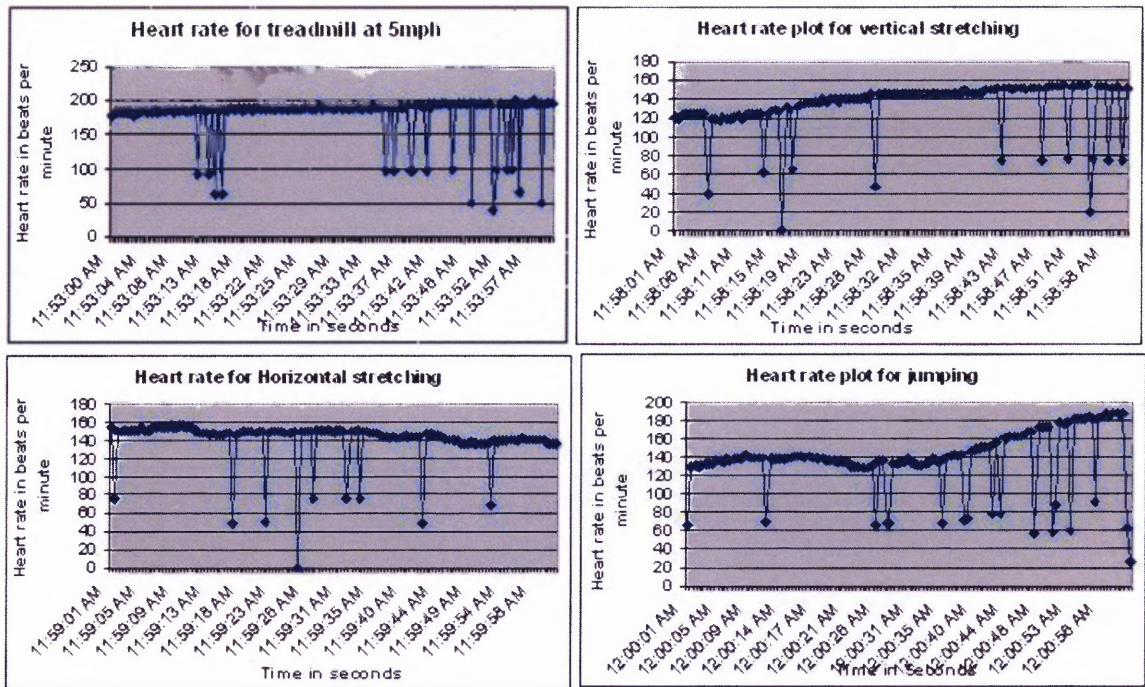


Figure 4.3 Heart rate plots for different activities (continued).

From these graphs the total number of R waves in the data and the number of missing R waves were analyzed. The noise might also be detected as an R wave under certain circumstances. But the second derivative condition of maximum negativity is not satisfied for noisy data. If noisy data was detected as R waves, the change would be visible in the heart rate plot. In that scenario, the heart rate plot would have data points above the graph pattern. No data points were observed above the graph pattern in any of the four subjects. Based on this it was concluded that no noisy data was detected as an R wave for all the four subjects. The missing R wave data is shown in Table 4.2 for four different subjects

Table 4.2 Total and Missing R Waves for all the Subjects

Activity	Subject 1		Subject 2		Subject 3		Subject 4	
	Missing	Tot	Missing	Tot	Missing	Tot	Missing	Tot
Sitting	1	68	4	110	3	87	1	85
Standing	3	74	4	114	6	100	5	86
Downstairs	4	58	5	137	12	98	2	100
Upstairs	4	140	11	138	20	81	4	124
Treadmill 1mph	4	116	10	134	12	96	11	97
Treadmill 2mph	2	127	8	136	13	96	4	103
Treadmill 3mph	10	139	7	148	15	92	6	109
Treadmill 4mph	12	155	20	143	23	93	3	127
Treadmill 5mph	16	163	26	137	15	32	16	127
Vertical Stretching	12	122	15	121	6	51	19	67
Horizontal Stretching	9	135	12	147	14	56	10	105
Jumping	17	126	17	80	4	27	5	58

From the data in Table 4.2 the percentage of good R wave data was calculated.

The percentage of good R waves was calculated using

$$\% \text{ good R waves} = (\text{Good R waves} / \text{Total R waves}) * 100 \quad (4.1)$$

This data shows that the number of missing R waves was increasing with increase in activity. This is due to large motion artifact during heavy activity. The percentage of good R waves for the four subjects for different tasks is shown in Table 4.3

Table 4.3 Percentage of Good R Waves

	Activity	Subject1 % good R waves	Subject2 % good R waves	Subject3 % good R waves	Subject4 % good R waves
1	Sitting	98.5	96.4	96.6	98
2	Standing	96.1	96.6	94.3	94
3	Downstairs	93.5	96.4	89.0	98
4	Upstairs	97.2	92.6	80.19	96
5	Treadmill 1mph	96.6	93.05	88	89.8
6	Treadmill 2mph	98.4	94.4	88	96
7	Treadmill 3mph	93.2	95.4	85.9	94.7
8	Treadmill 4mph	92.8	87.7	80	97.6
9	Treadmill 5mph	91.0	84	68	88.8
10	Vertical Stretching	91.0	88.9	89	77.9
11	Horizontal Stretching	93.7	92.4	80	91.3
12	Jumping	86.8	82.4	87	92

The plot of percentage of good R waves for the different subjects for different tasks is shown in Figure 4.4

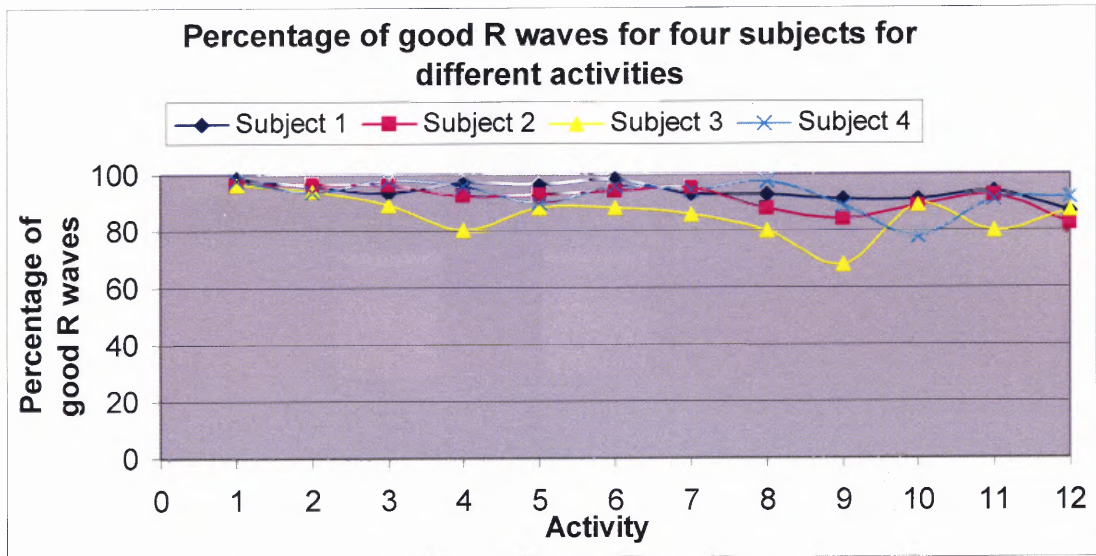


Figure 4.4 Plot of percentage of good R waves for different activities.

The mean of the percentage of good R waves and the standard error of the means were calculated for each subject and plotted. The graph is shown in Figure 4.5

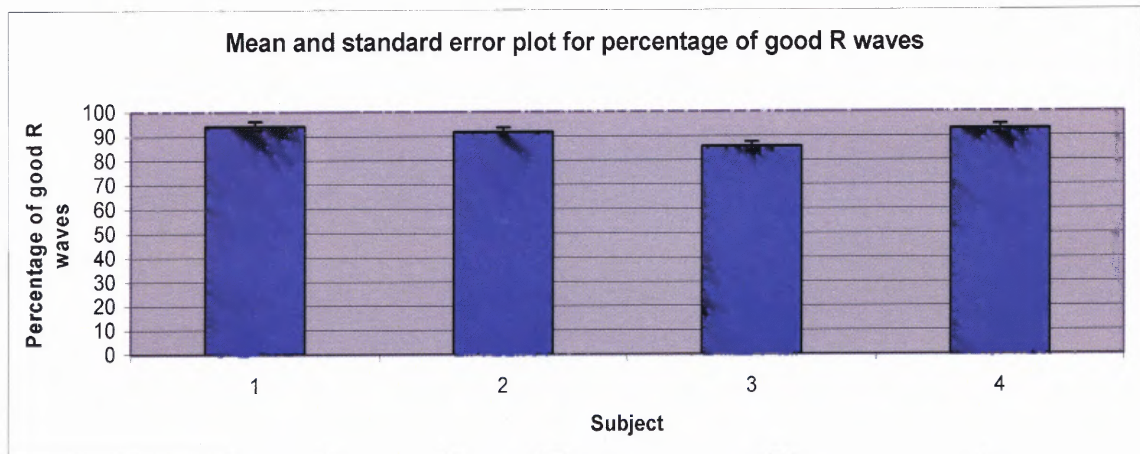


Figure 4.5 Mean and standard error plot for percentage good R waves

The graphs show that the heart rate was not calculated as accurately as in other activities during treadmill at 4mph and 5 mph and during vertical stretch because of large motion artifact.

4.2 Comparison of Standard and Ambulatory ECG

The simultaneously collected standard ECG data and the ECG data from the developed system were then analyzed. The correlation coefficients were calculated for each activity using standard and ambulatory ECG data. The correlation coefficients are shown in Table 4.4.

Table 4.4 Correlation Coefficients For Different Activities

Activity	Correlation coeff (subject1)	Correlation coeff (subject2)	Correlation coeff (subject3)	Correlation coeff (subject4)
Sitting	0.9218	0.800	0.85	0.404
Standing	0.9115	0.752	0.706	0.142
Treadmill 1mph	0.8594	0.697	0.4766	0.4715
Treadmill 2mph	0.8483	0.7617	0.404	0.265
Treadmill 3mph	0.7307	0.6892	0.354	0.4313
Treadmill 4mph	0.6407	0.604	0.2116	0.4325
Treadmill 5mph	0.5237	0.4745	0.0204	0.418
Vertical stretching	-0.19	-0.024	0.17	0.2963
Horizontal stretching	0.32	0.414	0.2441	0.2970
Standing still	0.66	0.6655	0.436	0.357

The plot of correlation coefficient with activity is shown in Figure 4.6

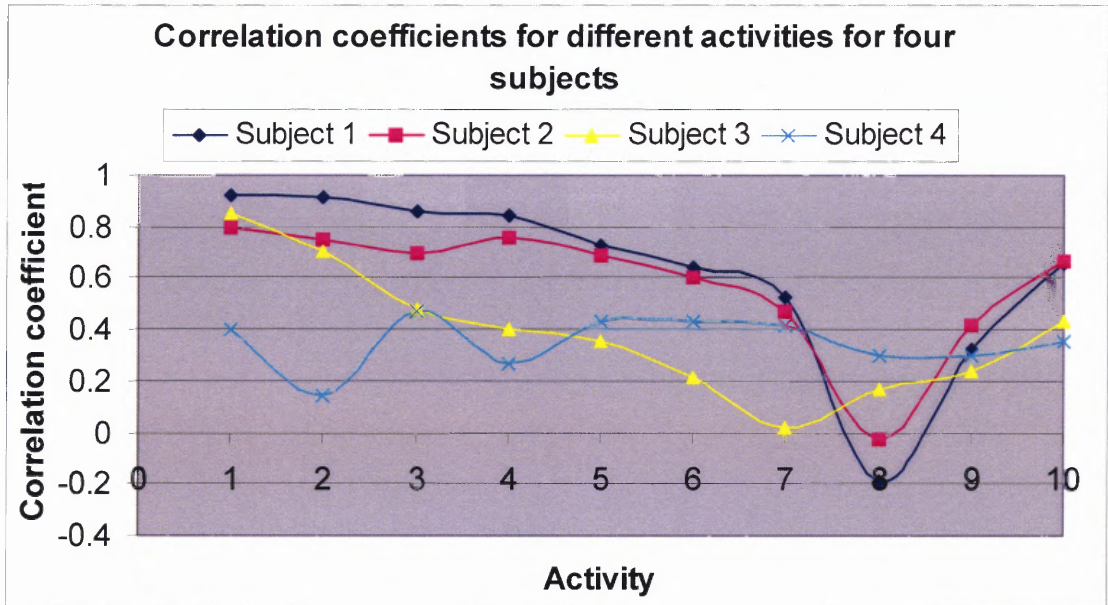


Figure 4.6 Correlation coefficients for different activities for four subjects.

The correlation coefficients were expected to be high. Some values were low because of the shifting of the ECG wave from the baseline for the standard ECG data. To verify the correlation coefficients, the standard ECG and the ambulatory ECG were plotted for different tasks for all the subjects. The graphs of subject 1 are shown in Figures 4.7, 4.8, 4.9, 4.10, 4.11.

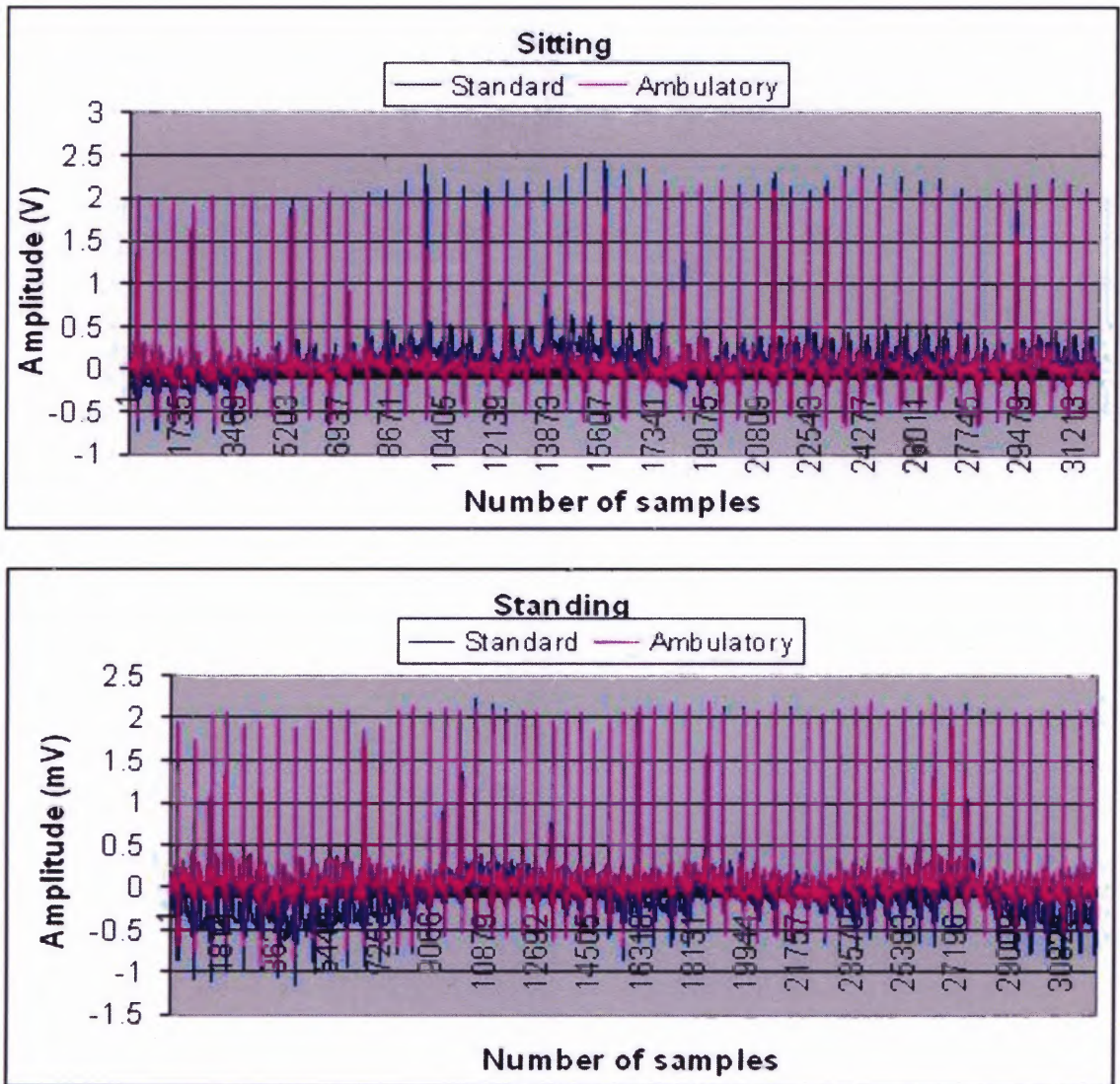


Figure 4.7 ECG graphs for standard and ambulatory ECG for different activities.

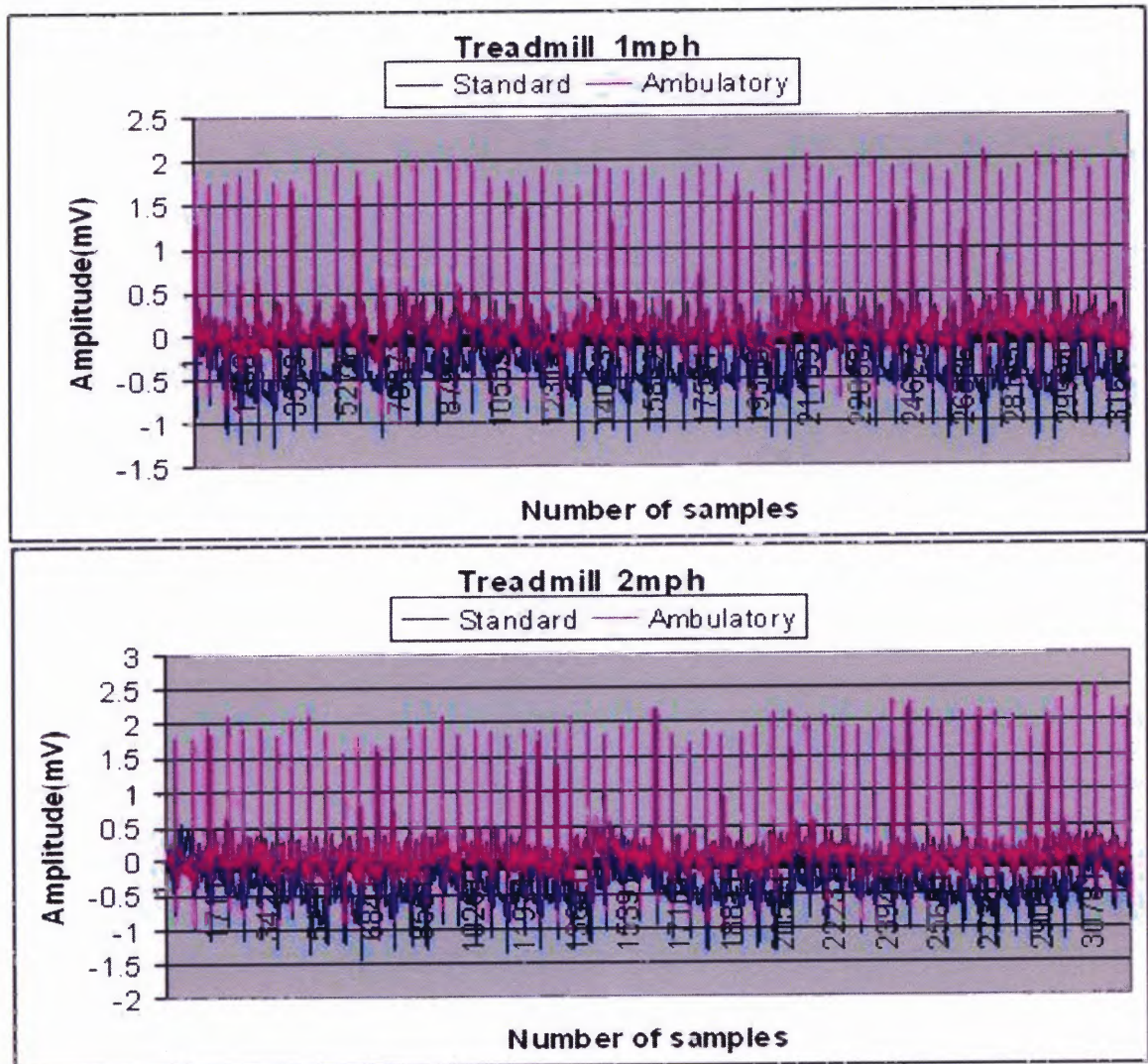


Figure 4.8 ECG graphs for standard and ambulatory ECG for different activities.

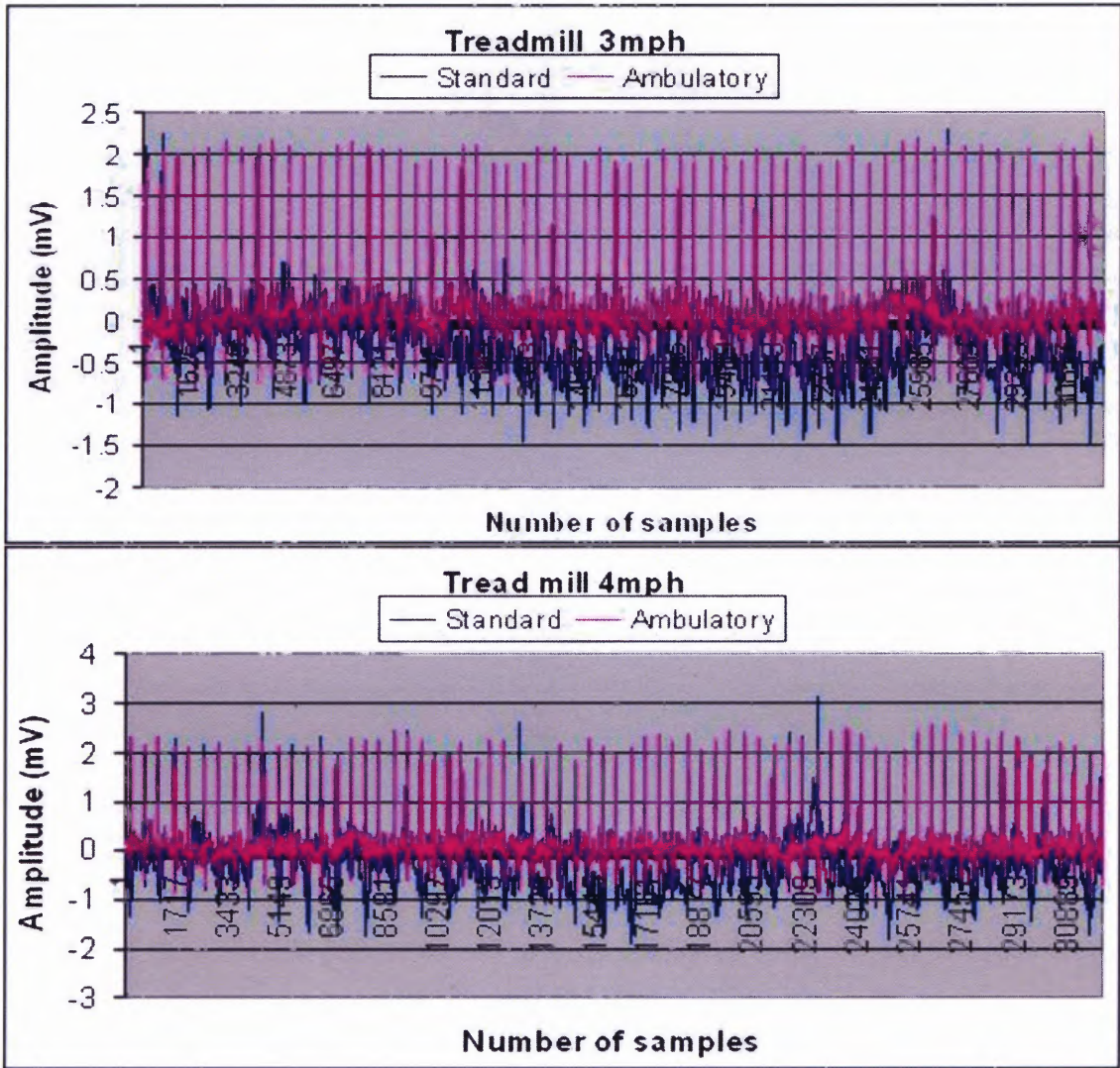


Figure 4.9 ECG graphs for standard and ambulatory ECG for different activities.

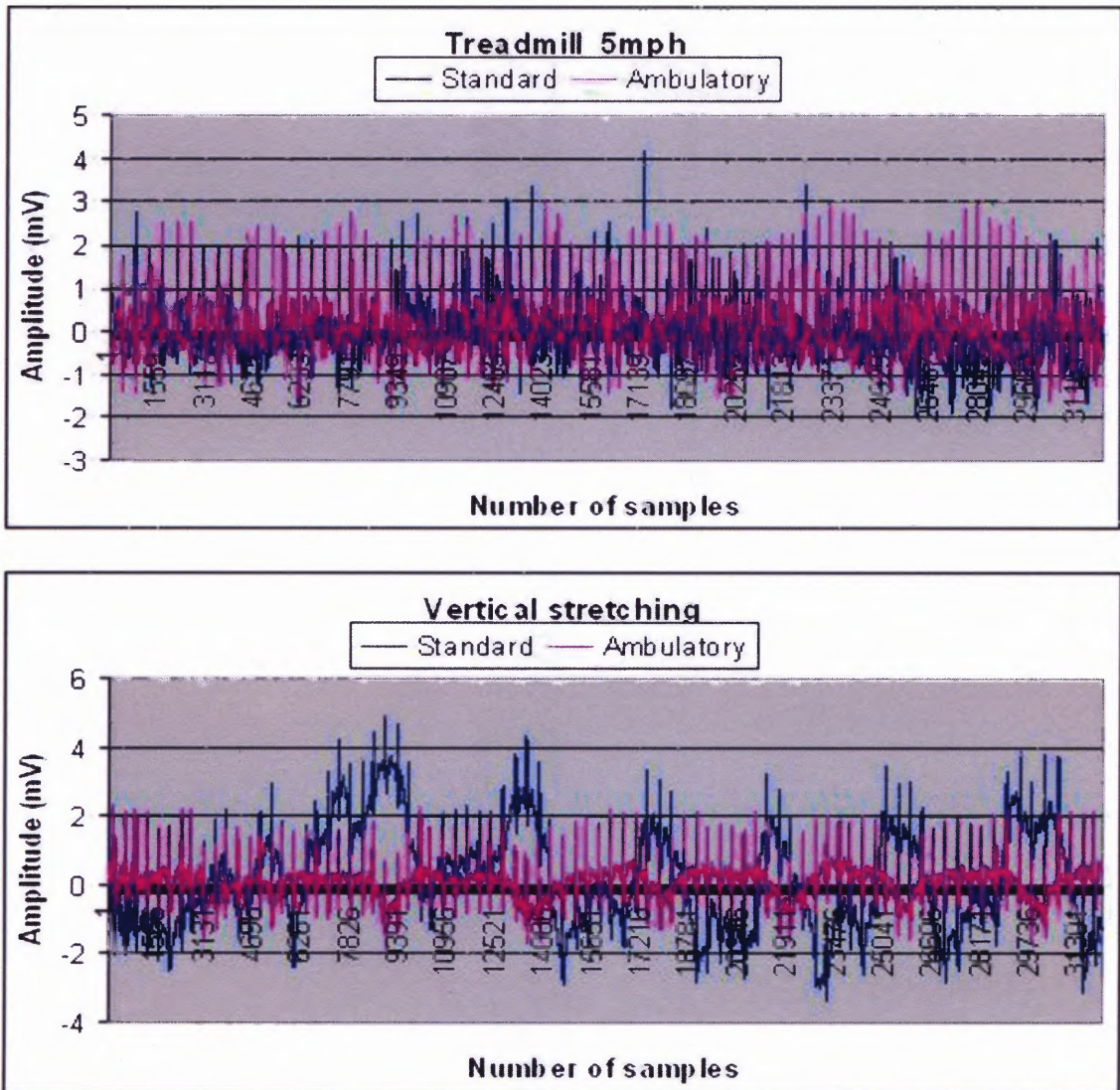


Figure 4.10 ECG graphs for standard and ambulatory ECG for different activities.

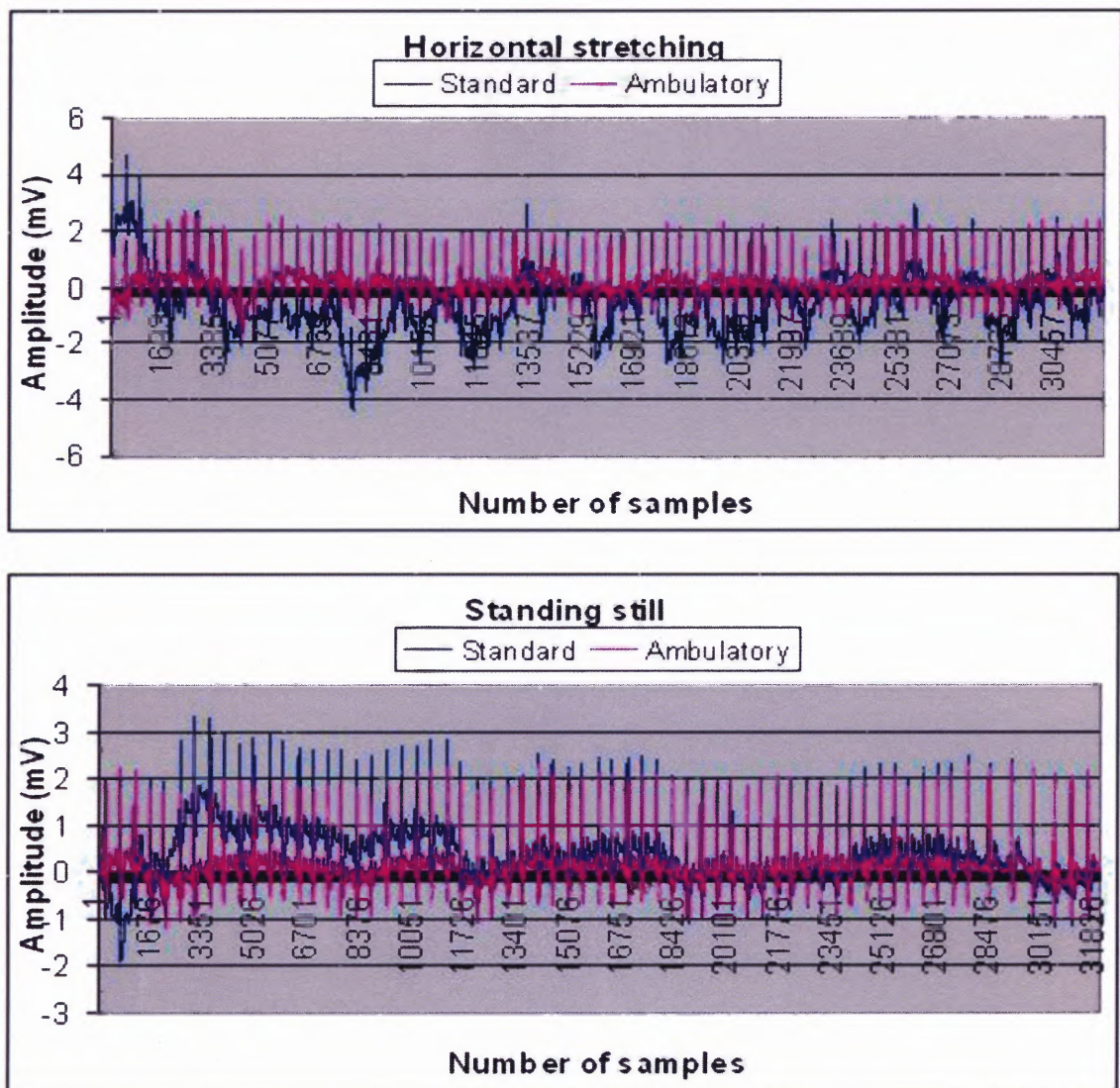


Figure 4.11 ECG graphs for standard and ambulatory ECG for different activities.

During heavy activity the developed system handled motion artifact better compared to the ECG data collected from the standard ECG machine. During less intensive activities described above the developed system was comparable to the standard ECG machine.

For subject 4 there was lower correlation coefficient. The reason was the shift in the standard ECG away from axis even when the subject was resting. For verification the

plot of standard and ambulatory ECG was plotted for subject 4 in the standing position.

The plot is shown in Figure 4.12

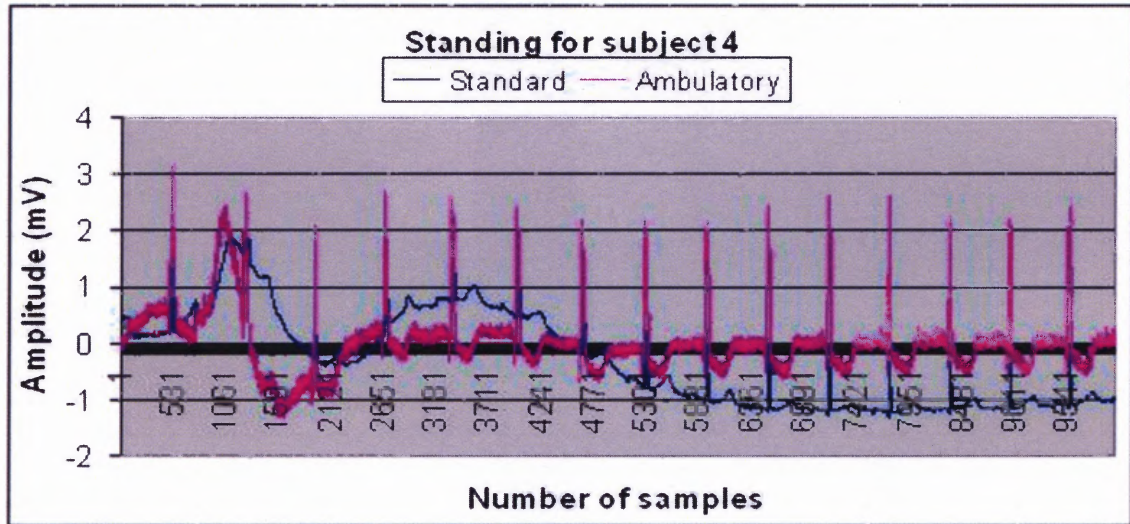


Figure 4.12 ECG graphs for standard and ambulatory ECG of subject4 when standing.

From this graph it can be observed that the correlation coefficient was small due to the shifting of the data from the axis.

4.3 Cost Analysis of the Developed System

The ambulatory biopotential devices present on the market cost up to \$10000. The life shirt system costs up to \$7000 [10]. The total cost of the developed system is shown in Table 4.5

Table 4.5 Cost Analysis

Device	Cost
Hp IPAQ pocket PC h555	\$519.99
PCMCIA card	\$695.00
Cable	\$45.00
Expansion pack	\$149.99
Connector	\$50.00
Total cost of hardware	\$30.00
Total cost of system	\$1489.98

The total cost of the system is only 21.2% of the cost of the present life shirt system available in the market.

4.4 Memory Capabilities

The pocket PC has a RAM size of 128MB and a ROM size of 48MB. Since the raw ECG data were collected at a sampling rate of 200 samples per second for 24 hours, it occupies 34MB since 1 sample occupies 2 bytes of memory. For 24 hours it was calculated as

$$\text{Memory} = 24 * 60 * 60 * 200 * 2 = 34560000 = 34.56\text{MB}$$

To store raw ECG data for an extended period of time, an additional memory card could be used in the PDA.

CHAPTER 5

DISCUSSION

The ambulatory systems currently on the market are expensive, bulky and the PDA's used for data analysis are outdated. With the development of a new era of electronics, new PDA models are emerging in the market, which are lightweight and inexpensive. To use the new PDA models in the present ambulatory systems like the Life Shirt, the company (Vivometrics) has to modify the PDA configuration and the interface. This makes the whole migration task expensive.

The developed system is cost effective, up to date in technology and has more flexibility for incorporating changes. It uses the recent IPAQ HP Pocket PC, DAQ card, cable and the expansion pack that are obtained off shelf. This makes the PDA upgrade to newer versions easy and inexpensive. Another advantage is the use of LabVIEW PDA software to collect the ECG data and detect R waves for ease of enhancements to the developed software. The cost of the whole system was the PDA, DAQ card, expansion pack, cable for DAQ card and the developed hardware, which was comparably cheaper than the existing ambulatory devices in the market.

It was a challenging task to make an ambulatory device that can analyze data real time, operate accurately, reliably and inexpensively. A lot of time in this project was spent building the system, developing the software, testing the system, collecting the data, and analyzing the collected data. In building the hardware, much research was done in selecting the filter cut-off frequencies for different biopotential signals.

Development of software was another important part of this project to analyze the ECG data in real time along with calculation of heart rate. PDA has 128MB RAM size. Care was taken not to use so many graphics that could reduce the speed of the process. The memory and battery life were considered carefully. The raw ECG data was stored simultaneously in the PDA.

The pilot data was collected primarily to determine whether the developed ambulatory system could record and store the biopotential signal and perform data analysis accurately and reliably while the person is sitting, standing, being on a treadmill at 1mph, 2mph, 3mph, 4mph, 5mph, climbing and going downstairs. In the experiment, the raw ECG data and heart rate were stored in the PDA along with time and date under different conditions. Then the standard ECG and ambulatory ECG were collected simultaneously in order to quantify the quality of the raw ECG data.

The results of the pilot experiment showed that ECG and heart rate were measured accurately with the developed system. The heart rate analysis showed that the number of detected R waves was decreasing with increasing activity. When the person is walking on a treadmill at 4mph and 5mph, the percentage of good R waves decreased due to motion artifact. The results demonstrated that the quality of 3 lead ECG was comparable to a standard ECG which costs up to \$15000 and it was handling the motion artifact more reliably than a standard ECG when a person is on a treadmill at 4mph, 5mph and while doing vertical stretching. Figure 4.8 shows that the ambulatory ECG was handling motion artifact better than the standard ECG machine.

CHAPTER 6

CONCLUSIONS AND FUTURE DEVELOPMENT

The main goal of this project was to develop a low cost and flexible ambulatory biopotential system compared to the commercially available ambulatory systems on the market like the Life Shirt, to write a software program that would acquire, display, store and process data online and to analyze the data to confirm accuracy of the system. Based on the goals that were originally set, this project was a successful one. We were able to develop a system that is inexpensive and could work under day-to-day activities such as sitting, standing, being on a treadmill at different speeds, climbing stairs and going downstairs and jumping.

Through a series of tests, the system was shown to be accurate and reliable. The pilot experiment was called accurate because of a comparison of the collected data to a standard ECG machine. It was reliable because this pilot experiment gave similar kinds of results when repeated in similar environments. The developed system has the capability to store the heart rate data and raw ECG along with date and time for up to 24 hours with the use of a separate memory card.

However, the system has certain limitations. One limitation was the expansion pack battery. Though the battery life of the hardware and PDA is up to 24 hours the expansion pack battery is limited. Possible solutions could be

- To replace it by an external battery for 24 hour operation.
- To avoid the use of the expansion pack by building an A/D converter by other circuitry.

The other limitation was the increase in number of missing R waves during heavy activity. The solutions could be

- Using a higher order filter in the hardware
- Use of a better R wave detection algorithm
- Use of software filter

The present technology does not support software filtering in LabVIEW PDA. It could be further implemented. Potential future enhancements for this project could be to extend the real time analysis for other biopotential signals.

REFERENCES

- [1] Version 7.1 (National Instruments; Austin, TX). <http://www.ni.com/labview> (July, 2003).
- [2] Purdue University. BioMedia Center (General Biology Laboratory Manuals). <http://biomedial.bio.purdue.edu/GenBioLM/index.html>. (June, 2004).
- [3] R. Lewis, *Life*, Wm. C. Brown Communications, Dubuque, IA, 1995.
- [4] J. B. Webster (ed.), *Medical Instrumentation: Application and Design*. 3rd ed., New York: John Wiley & Sons, 1998.
- [5] A. C. Guyton, *Structure and Function of the Nervous System*, 2nd ed., Philadelphia: W. B. Saunders, 1972.
- [6] RCN Corporation (2004). Muscles. <http://users.rcn.com/jkimball.ma.ultranet/BiologyPages/M/Muscles.html> (October 24, 2004).
- [7] Computer assisted teaching system (2003). Gastrointestinal system. http://physioweb.med.uvm.edu/gi_physiology (October, 2004).
- [8] Medicine net (1996-2004). Electrogastrogram. <http://www.medicinenet.com/Electrogastrogram/article.htm> (October, 2004).
- [9] D. Buckles, F. Aguel, R. Brockman, J. Cheng, C. Demian, C. Ho, D. Jensen, E. J Mallis. "Advances in Ambulatory Monitoring: Regulatory Considerations". *Electrocardiol.* 2004; 37 Suppl: 65-7.
- [10] Vivometrics Inc (1994-2004). Lifeshirt System. <http://www.vivometrics.com/site/pdfs/find.php?file=wpLifeShirtReview> (March, 2004).
- [11] HowStuffWorks. Inc (1998-2004). How PDA works. <http://electronics.howstuffworks.com/pda1.htm> (October, 2004).
- [12] New Jersey Institute of Technology (2004). Biopotential signals. <http://www.njit.edu/bme/Classes/Mr.Bergen/BME687/BME687%20-%20Biopotential%20Signals.pdf> (December, 2003).
- [13] T-linespeakers (2004). Sallen-Key filter. <http://www.t-linespeakers.org/tech/filters/Sallen-Key.html> (December, 2003).

- [14] Jupiter Media Corporation (2004). DIP switches.
http://www.webopedia.com/TERM/D/DIP_switch.html (December, 2003).
- [15] G. Rudolph, Encyclopedia of Electronic Circuits, vol 3, p 403.